People's Democratic Republic of Algeria

وزارة التعليم العالي والبحث العلمي

Ministry of Higher Education and Scientific Research

جامعة الجيلالي بونعامة خميس مليانة

Djilali Bounaâma University of Khemis Miliana

Faculty of Science and Technology

Department of Material Sciences

End of study dissertation

With a view to obtaining a Master's degree in material sciences

***Specialty**: theoretical physics*

Theme:

Ground state study for spin-3/2 Ashkin-Teller model on hypercubic lattice.

Presented by:

Zerrouki chaima

In front of the jury composed of:

- Ouerdane Abdellah President
- Yezli Mohammed Framer
- Boudjema Fatiha Examiner

College year: 2022 / 2023

Acknowledgements

I am truly grateful for all the support, encouragement, and guidance I have received throughout my academic journey. It has been a long and challenging road, but with the help of my family, my dedicated teachers, and my fantastic colleagues, I was able to achieve my goal of graduating. I couldn't have made it this far without their unwavering belief in me and their willingness to go the extra mile, whether it was staying up late to help me prepare for an exam or just being there to offer words of encouragement when the going got tough. Graduation is a day of celebration, not just for me, but for all those who have supported me along the way. I am proud to have been a part of this incredible community, and I know that I will take the lessons, values, and friendships that I have gained during my time here with me as I embark on the next chapter of my life. Thank you to everyone who has played a part in making this moment possible.

I would like to warmly thank the members of the jury, Mr. Pr. Ouerdane Abdellah and Mrs. Dr.Boudjema Fatiha , for their contribution to the evaluation of this work.

I would also like to thank the teachers of the Department of Matter Sciences in my "Theoretical Physics" branch for their efforts to ensure our success.

My framer teacher Dr, M. Yezli was a great mentor in learning the skills and techniques of framing. He was patient and encouraging, always willing to share his knowledge and expertise with me. Under his guidance, I learned technical skills and a lot of scientific pieces of information, He would often remind me that should do my own print in our work. He encouraged me to take my time, be creative and always strive for excellence..

I am grateful for the time I spent learning from my framer teacher, and his influence has significantly impacted my career in the future.

Mom and Dad, your constant prayers and motivation kept me going whenever I felt like giving up. You both always reminded me of the importance of education and encouraged me to strive for excellence. Your sacrifices to provide me with the best education possible will always be appreciated and never forgotten. As I graduate today, I am proud to say that I did it with the love and support of my fantastic family. Thank you for everything you have done for me, and for always being there. Your support has significantly impacted my life, and I will always be grateful.

الملخص:
درسنا نموذج الدوران الشبكي، وهو نموذج Askhin-Teller على Hypercubic ، من خلال إدخال spin S=3/2. أظهر الرسم التخطيطي لمرحلة الحالة الأرضية مراحل جديدة ظهرت في مناطق مختلفة من الرسم التخطيطي ببنية لا تختلف كثيرًا عن الرسوم التخطيطية الأخرى تم العثور عليها باستعمال قيم S أقل. يتم فصل هذه المناطق باستخدام انتقالات طور من الدرجة الأولى.

كلمات رئيسية:
نموذج Askhin-Teller (ATM) ; تدور S = 3/2 ; شبكة .Hypercubic ; رسم تخطيطي لمرحلة الحالة الأولية.

Abstrat:
We studied a lattice spin model, namely the Askhin-Teller model on a hypercubic lattice, by introducing the spin S=3/2. The ground state phase diagram showed new degenerate stable phases that appeared in different regions of the diagram with a topology that is not so different from others found for lower spin orders. These regions are separated with first-order transitions.

Keywords:
Askhin- Teller Model (ATM); Spin-3/2; Hypercubic lattice; Ground state phase diagram.

Résumé :
Nous avons étudié un modèle de spin sur réseau, à savoir le model d'Askhin-Teller sur un réseau hypercubique, en introduisant le spin-3/2. Le diagramme de phase de l'état fondamental a montré de nouvelles phases qui sont apparues dans différentes régions du diagramme avec une topologie qui n'est pas si différente des autres trouvés pour des ordres de spin inférieurs. Ces régions sont séparées avec des transitions du premier ordre.

Mots clés :
Le modèle d'Askhin Teller (ATM) ; spin-3/2 ; Réseau hupercubique; Diagramme de phase de l'état fondamental.

Table of contents

General Introduction

Statistical physics is a branch of physics that aims to study systems made up of identical elements. This approach is more important when the number of these constituents is large enough that calculating averages over them is more or less interesting than studying them individually. For example in a glass of water, there is about 10^{29} molecules; storing the positions of each of these molecules would require at least minus one hundred billion common 100 GB computer hard drives, i.e. well more than the number of humans present on earth, so we can only calculate properties average or typical, so it becomes very expensive or even humanly impossible to study them separately.

This emphasizes a spectacular aspect of the phenomena studied by statistical physics: the overall behaviour of all the constituents seems completely detached from the laws that govern them. The laws of the microscopic movement of water molecules are strictly the same at 99° C and at 101° C, but we have the impression of dealing with two different bodies (a liquid and a gas), governed by different laws. How can we believe that such a small change in temperature has such a great consequence on the macroscopic behaviour of matter?

A type of macroscopic behaviour is additionally called a phase and the transition from one to the other is a phase transition. Part of the task of statistical physics is to identify, characterize and classify these phases

The study of the magnetic properties of materials requires the use of calculation and simulation methods capable of probing matter at the atomic scale while explicitly taking into account the electronic structure of chemical elements. The methods theory prove to be the tools of choice for modelling materials at the atomic or even electronic scale, and for direct access to a set of fundamental data such as the magnetic properties of materials. Among these theoretical methods, we cite approximate methods such as the effective field theory, and exact methods such as the transfer matrix method, widely used for two-dimensional models and the Monte-Carlo method.

This work consists of three chapters followed by a general conclusion. We will give some properties on magnetism in a first part; we will explain in detail the phase transitions, their classification and the critical phenomena that accompany a continuous transition. In the second chapter, we will review the different methods used in statistical mechanics. We will give more interest to exact methods, namely the Monte-Carlo method and the transfer matrix method. In the last part, we will present our studied system, with necessary interpretations, which is the Ashkin-Teller model known by the abbreviated name: the ATM model. We will end with a general conclusion and the perspectives for the future.

Chapter 1

1.1. Introduction

In this chapter, we give a general definition of magnetism and phase transitions in the context of statistical physics, in which we will become familiar with the theory of statistical mechanics, such as the principles of statistical physics and the properties it has. We also discuss some fundamental concepts related to the magnetism of materials, such as the origin of magnetism and different types of magnetism. We will then introduce some basic concepts of phase transition theory, classifying phase transitions and then some ideas from Landau's theory that lead to critical phenomena.

1.2. Theory of statistical mechanics

1.2.1. Principles of statistical physics

In classical statistical mechanics, all particles positions and spins must be the same. Many particles with many possible spins and positions exist in theory but most classical systems do not involve them. Instead, these theories focus on systems with just a few degrees of freedom. The systems available ranges of motion are represented by the spaces between each degree of freedom. These spaces are referred to as phase space, and any point within them is indicative of the systems present state. The paths the system follows in phase space are dictated by the equations of motion. Thermometers and barometers measure slowly, so their measurements of physical quantities like pressure take time. This is why only measuring devices respond slowly can measure only the average time of an interest physical quantity. [1]

Understanding the physical properties of a substance through statistical mechanics is crucial to many fields of study. Matter is defined by the constant operation of its individual parts. "Statistical principles relating to micron size" on the other, this word is considered a configuration of the original phrase. In addition to the Hamiltonian approach, statistical mechanics also utilizes the principles of mechanics derived from statistics. Its value as a science asset has been recognized for years. A fundamental understanding of this subject is necessary to his pursuit. We can use any physics study for any purpose. For instance, we might want to learn about astronomy. Specialize in a specific subject matter. This school of thought encompasses nearly every subject. It’s theoretically capable of addressing any state of matter, naturally occurring phenomena. More specifically, it refers to the use of matter in a solid, liquid or gaseous state as well as being studied. Mixture of many components and phases of material [2].

1.2.2. Theory of statistical mechanics

In basic statistical mechanics, it starts with the canonical partition function [3]:

$$Z(T,H) = \sum_r e^{-\beta E_r} \tag{1.1}$$

Where the sum over all the states r with E_r is given by

$$\beta = \frac{1}{KT} \tag{1.2}$$

Where k is Boltzmann's constant and T is the temperature, although this is not the case for magnetic systems, so it is convenient to consider an ensemble where Z depends on the temperature and the field H. The Maxwell-Boltzmann statistic is appropriate because the magnetic system we consider consists of localised and thus distinguishable spins, and the fluid system is in the classical state.

The partition function is proportional to the free energy:

$$F(T,H) = -KT\ lnZ \tag{1.3}$$

The calculated properties of any system can be found by subtracting free energy from a larger amount. This is demonstrated in equations 1.1 and 1.3 for magnetic and fluid systems. Also, it's possible to calculate the free energy by focusing on that aspect of an equation. However, many equations aren't easier to calculate properties like magnetism or energy in that aspect. [4]

1.2.3. Macroscopic and microscopic states

We consider a physical system composed of N identical particles conned to a space of volume V. In a typical case, N would be an extremely large number generally, of order 10^{23}. In view of this, it is customary to carry out analysis in the so-called thermodynamic limit, namely $N\rightarrow\infty$ and $V\rightarrow\infty$. The extended properties of the system take place within this boundary. Size-based, in other words proportional to N or V [5]. Longer or shorter systems don't change their proportion. Determining the overall density of a substance remains unchanged regardless of its independence of properties, which are intensive. The energy represented by E is the sum of all energies represented by ε_i individual particulates [6].

$$\boldsymbol{E} = \sum_{\boldsymbol{i}} \boldsymbol{n_i}\, \boldsymbol{\varepsilon_i} \tag{1.4}$$

Where n_i denotes the number of particles each with energy ε_i

$$N = \sum_i n_i \tag{1.5}$$

1.2.4. Magnetic properties of Martials

Technological devices now require magnetic materials as a part of their construction. Some examples of devices that use magnets include cars and appliances. More than fifty devices in a typical home contain magnets; ten can be located only in a standard family car [7]. Permanent magnet materials are essential to many medical and industrial devices. They're used as components in machines that store the energy. Also, information technology uses magnetic materials to perform multiple tasks. Many of these tasks involve moving electrical and mechanical energies between each other or transferring force to magnetic materials [8].

In the context of quantum physics, electrons possess certain properties that contribute to their magnetic pull. The first part is of the spin of electrons (spin magnetism); the second is motion around the atomic nucleus (orbital magnetism). The last two parts of magnetic pull are related to the nucleus itself (nuclear magnetism) and are used in medical imaging techniques [11]. Magnetic fields in the universe result from moving electric charges. Force acting on these charges, known as Lorentzian electromagnetic forces, is a manifestation of magnetic fields [10]. The magnetic field formed is the impetus behind its rotating spin on its axis (the magnetic quantum being Bohr's magnetrons). It can be read as a sign of movement when observed via a magnet, whether it's moving upward or downward. A pair of electrons can't occupy the same orbital path unless one revolves counter to the others motion with opposite magnetic polarity (Pauli's Principle).

Large distances in space contain magnetic fields with distinct north and south poles. Many magnetic fields combine to create larger ones that rotate around the same direction. Many moments of magnetism can be seen at this larger scale. Many magnetic fields at a larger scale.

Can become magnetized regions where all these moments align in the same direction [11]. These regions of space are separated from each other. At the macroscopic scale, these areas are magnets thanks to the walls that surround them. When the domains are grouped together, they can also create a large macroscopic magnetic [12].

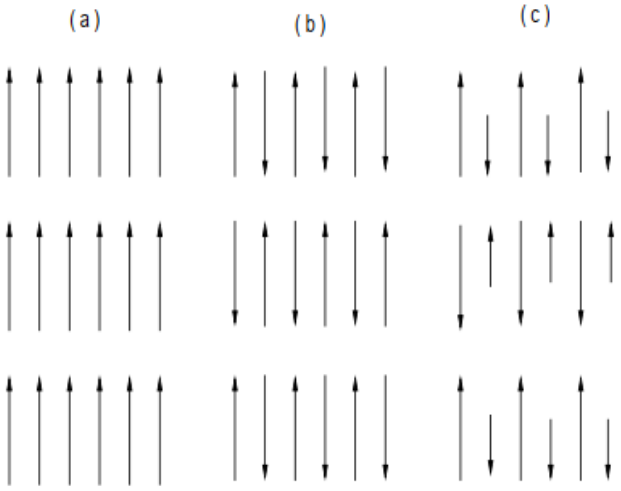

Figure 1.1: Elementary magnetic moments in different substances: (a) ferromagnetic substances, (b) anti-ferromagnetic substances and (c) ferromagnetic substances.

1.2.5. Magnetization and susceptibility

1.2.5.1. Intensity of Magnetization

To describe the magnetic properties of materials [13] one must pass by the calculation of the average of all their magnetic dipoles on a specific volume. The sum of all the dipoles forms the magnetization of the sample represented by the vector M. The macroscopic magnetic solid of M has an edge where local variations due to atomic magnetic moments or time-scale fluctuations are ignored. Instead, the smooth vector field is only considered when all magnetic moments of M are parallel to each other. This is known as the continuum approximation. When M is at its maximum value, this is referred to as saturation magnetization M_S.

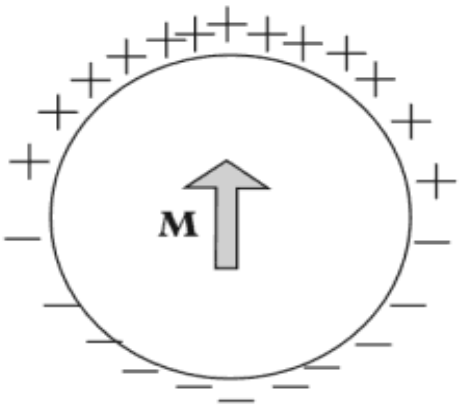

Figure 1.2: Distribution of magnetic "poles" for uniformly magnetized sphere with magnetization M

1.2.5.2. Magnetic susceptibility

Magnetic materials are usually classified according to their temperature dependent response to an applied field. To facilitate a quantitative comparison of this response and to classify materials into different magnetic classes, the magnetic susceptibility, noted by χ is defined as the ratio of the magnetization of the sample to the applied magnetic field. In the special case of linear materials, the magnetization M is linearly related to the applied magnetic field. The magnetic susceptibility is given by:

$$\chi = \frac{M}{H} \tag{1.6}$$

The relation between magnetization and susceptibility can be expressed as follows by:

$$M = \chi . H \tag{1.7}$$

A magnetic induction field B is generated in materials under the influence of an external magnetic field H as follows:

$$B = \mu H \tag{1.8}$$

With μ being a proportionality constant called magnetic permeability. The unit of magnetic induction is the Tesla (T). The magnetic field H, usually produced by the flow of an electric current in a solenoid, is measured in amperes per metre (Am^{-1}) and the magnetic permeability is expressed in Henry parameters (Hm^{-1}).

The magnetic permeability of matter can also be expressed as:

$$B = \mu_0 (H + M) \tag{1.9}$$

μ_0 is the magnetic permeability of the vacuum (μ_0=4m107Hm).

Alternatively, magnetic susceptibility is a material property. Since M and H have the same dimensions, χ is dimensionless. We can use equation (1.7) in conjunction with equation (1.9) to obtain

$$B = \mu_0 H(1 + \chi) \tag{1.10}$$

Thus, $1 + \chi$ represents the proportionality of the H category:

$$\mu = 1 + \chi \tag{1.11}$$

With 'u' being the magnetic permeability. Equations (1.8) and (1.9) show that

$$B = \mu\mu_0 H \tag{1.12}$$

Either μ or χ can be used to characterise a material, although engineers are generally interested in materials with large values of χ and μ. Engineers are more interested in the magnetic induction produced by a material than its magnetisation. Materials of practical interest are therefore generally characterised by their permeability.

1.3. Classification of magnetism

1.3.1. Diamagnetism

For all materials[13], there is a weak and negative contribution linked to the deformation of the electronic orbitals under the influence of a magnetic field and which is independent of temperature; it's diamagnetism. Diamagnetic materials have an extremely low negative magnetic susceptibility varying between 10^{-6} and 10^{-5}. There are several diamagnetic materials; the best known are: copper, silver, gold, graphite, quartz... All materials possess a degree of diamagnetism, which reverses when the exterior magnetic field disappears [14].

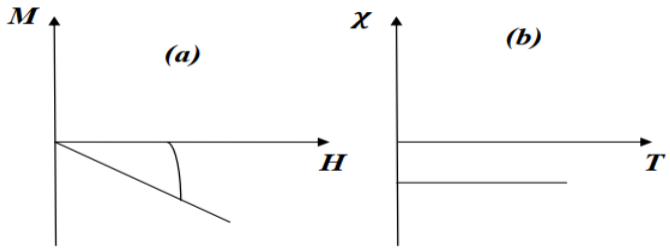

Figure 1.3: Evolution of M and χ as a function of respecchorely (field and temperature)

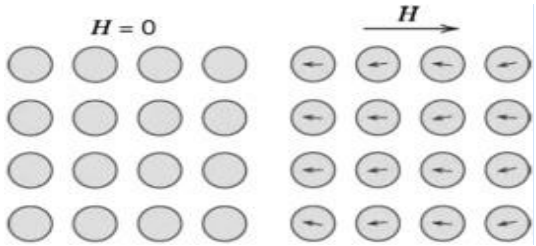

Figure 1.4: Alignment of electrons opposite the magnetic field (H)

1.3.2. Paramagnetism

Paramagnetism exists when the magnetic moments of atoms are present and are oriented in all directions. In this type of material, atoms or ions have unpaired electrons in partially filled orbitals. [13] This means that in a paramagnetic substance, each atom has a small net magnetic moment. If a magnetic field is applied, the magnetic moments align along its own direction, the magnetization of a paramagnetic material is lost when the field is suppressed due to thermal effects, so in this case, and in the absence of the external field, the overall magnetization is zero, for most so-called paramagnetic materials and under reasonable conditions of temperature and magnetic field exterior, the magnetization M of the paramagnetic material is proportional to the applied field H. The associated susceptibility often varies inversely proportional to the temperature; it is positive and weak and dependent on the temperature (according to the so-called Curie law) at room temperature it varies from the order of 10^{-4} to 10^{-5}.

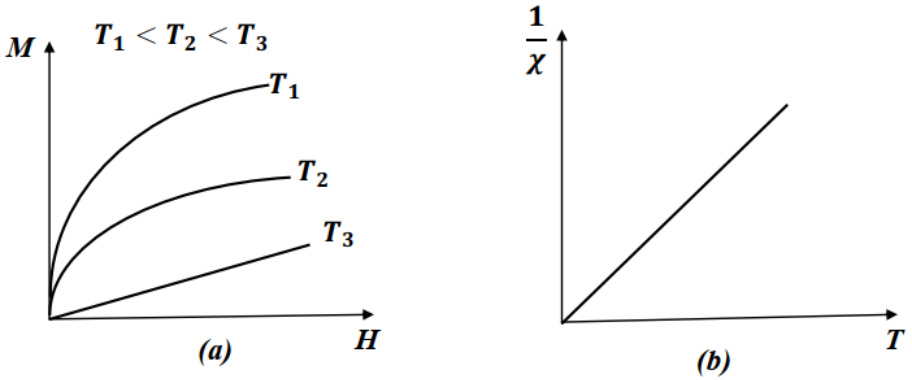

Figure 1.5: Paramagnetic behaviour present (a): magnetization as a function of magnetic field. (b): Inverse of susceptibility as a function of temperature.

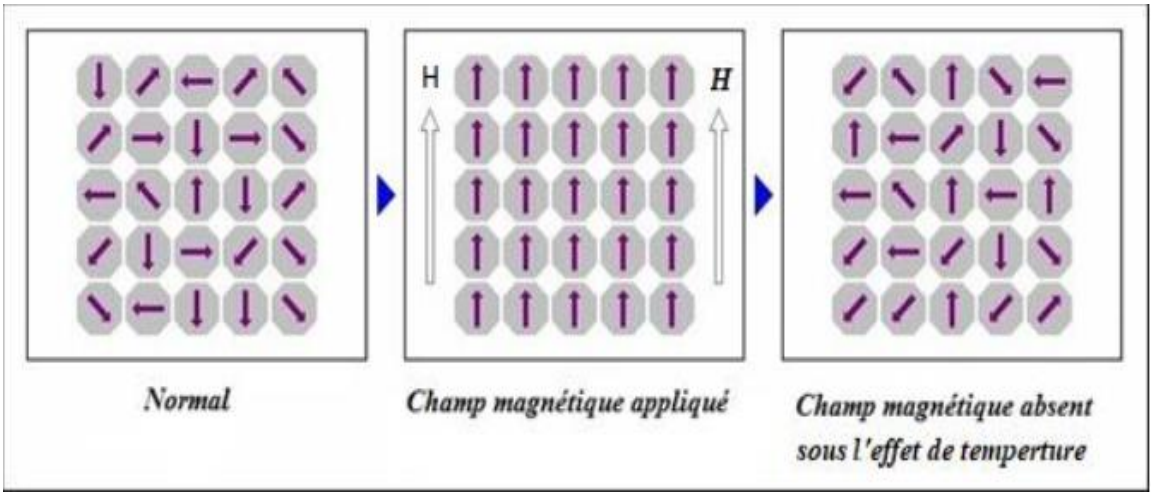

Figure 1.6: Paramagnetic materials

1.3.3. Ferromagnetism

Ferromagnetic materials are made up of atoms with strong permanent magnetic moments, the spins of two neighbouring electrons are oriented in such a way that a strong interaction develops between the atoms containing these electrons. The magnetic moments are aligned parallel as shown in the figure (1.8).

These magnetic moments are aligned parallel to each other and retain magnetization even in the absence of the external field, and in order to minimize the free energy of the system, the material is divided into domains having spontaneous magnetization. In Indeed, the magnetization of such a material decreases when the temperature increases to cancel out at an order/disorder transition temperature: characteristic called temperature by Curie T_C [13].

Ferromagnetic materials lose their special properties above Tc. The Curie temperature is the temperature at which a ferromagnetic material becomes paramagnetic under the influence of a temperature rise. Below the Curie temperature, the ferromagnetic interactions tend to align parallel. Neighbouring magnetic moments in the material. However, by increasing the temperature, the spins fluctuate rapidly. This process is reversible because the ferromagnetic order reappears in the system when its temperature drops below the Curie temperature whose value varies from one material to another.

Inferior-quality magnetic materials exhibit M which is not a single-valued function of the applied H. This phenomenon is called hysteresis and is commonly seen in ferromagnetic and ferromagnetic. When an outside source of force is applied, all of the materials magnetic domains point in the same direction. This is referred to as magnetization alignment or saturation magnetization. It is the highest achievable level of magnetization in any direction. Increasing the temperature maintains hysteresis behaviour. However, the magnetization value decreases until a level is reached where the thermal energy is enough to counterbalance strong magnetic interactions between materials. This is known as the Curie temperature, or Tc, for the materials magnetism. From that point onward, the magnetization value of the material decreases until zero saturation magnetization occurs. Of course, the Curie temperature is a measure of the strength of interactions between magnetic moments of atoms in a given material. At temperatures T >Te, the sample effectively exhibits paramagnetic behaviour and obeys the ferromagnetic Curie-Weiss law:

$$\chi = \frac{C}{T - T} \tag{1.13}$$

It is clear that the magnetic susceptibility χ diverges at the Curie temperature T_C when approached from above. However, one more word of caution is necessary. Recall that for Ferro-magnets, the magnetic field inside the object is $H_{int} = H_{app} - N_d M$. It is the intrinsic magnetic susceptibility of the material, $\chi_{mat} = M/H_{int}$, diverging at T_C [15].

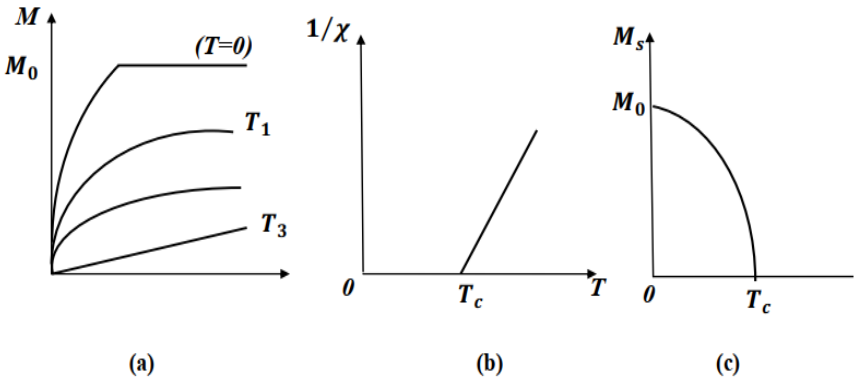

Figure 1.7: a) Magnetization field dependence (Ti <TC<T2< T3), b) Temperature dependence of $1/\chi$ c) Temperature dependence of spontaneous magnetization

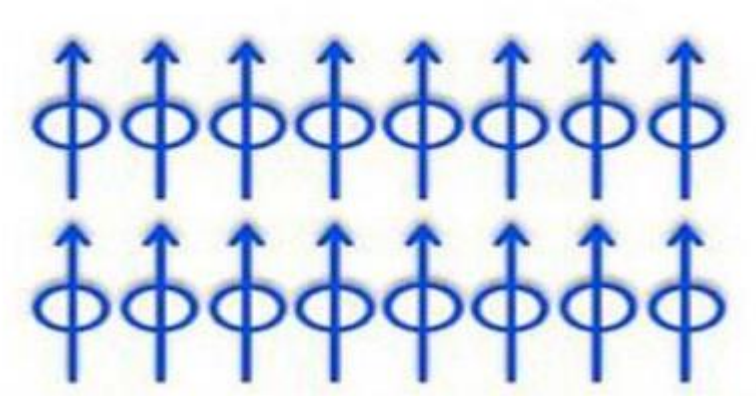

Figure 1.8: Ferromagnetic materials show a parallel alignment of moments

1.3.4. Anti-ferromagnetism

Certain materials have magnetic properties due to the way their atoms are arranged. Typically, these materials have repelling magnetic forces between the atoms that make up the material. Only a single magnetic species is present; it's evenly distributed in two intersecting but antiparallel lattices that form a honeycomb structure. When perfectly aligned, the materials exhibit no magnetism because the single magnetic species cancels out any spontaneous magnetization. Some materials exhibit weak or no magnetism at room temperature; however, they become paramagnetic at a specific temperature - typically below 0°C - T_N (Néel temperature). Subscripts H∥and H⊥Indicate the direction of spin lattice propagation through the material. Below T_N, susceptibility to a field is dependent on the direction of applied magnetism. When applied in parallel, or $H_{\parallel}$, to the spin-lattices direction of propagation, susceptibility increases; when applied perpendicular to the spin-lattice direction of propagation, susceptibility decreases. A function of this phenomenon is shown in Figure. The temperature dependence of antiferro-magnetism, $T>T_N$, is derived from equations that accept T as input and TN as output. These equations state that the susceptibility rises linearly with temperature until reaching a maximum and then declines until reaching a minimum:

$$\chi = \frac{C}{T-\theta} = \frac{C}{T-T_N} \qquad (1.14)$$

T_N is the temperature of Néel and θ=-T_N is the intercept of $1/\chi$,

For T>T_N, when extrapolated on the temperature axis.

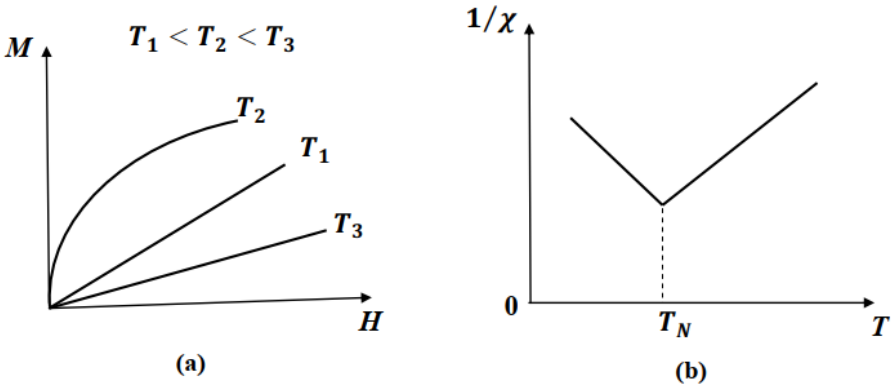

Figure 1.9: a) dependence of magnetization as a function of magnetic field b) inverse of susceptibility as a function of temperature

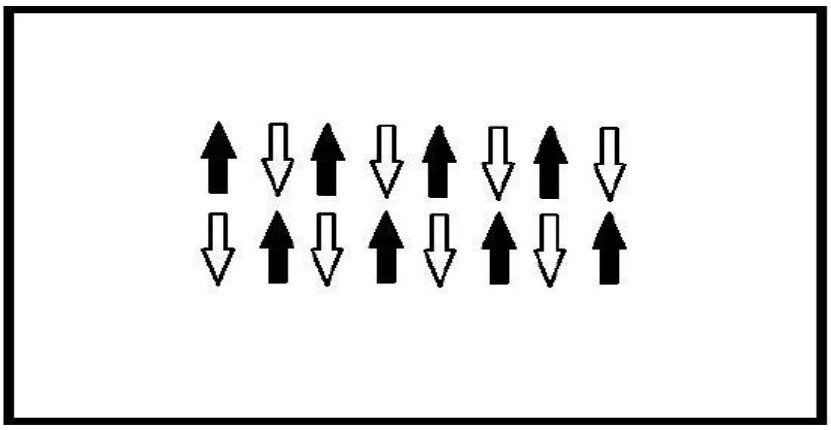

Figure 1.10: Antiferromagnetic arrangement

1.3.5. Ferrimagnetism

This behaviour is usually observed in materials (usually oxides) with two or more magnetic species occupying different sub lattice positions and having different magnetic moments. There is a strong negative interaction between the two sub lattices, resulting in an antiparallel alignment. However, in contrast to antiferromagnets, ferrimagnets show spontaneous magnetization below the Curie temperature Te when the two sub lattices are ordered [15].

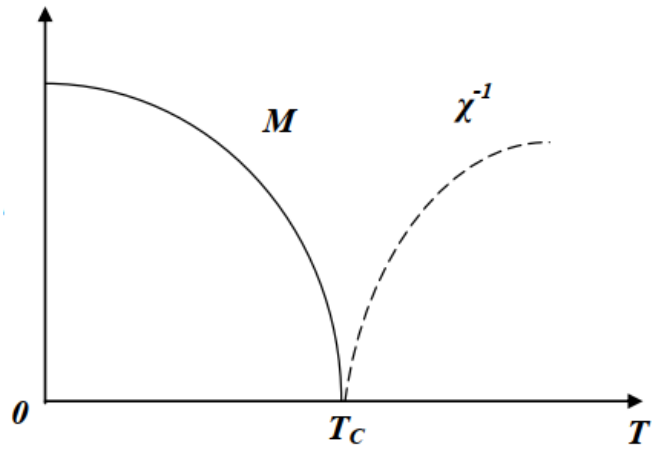

Figure 1.11: Two quantities present the ferri-magnetic behaviour.

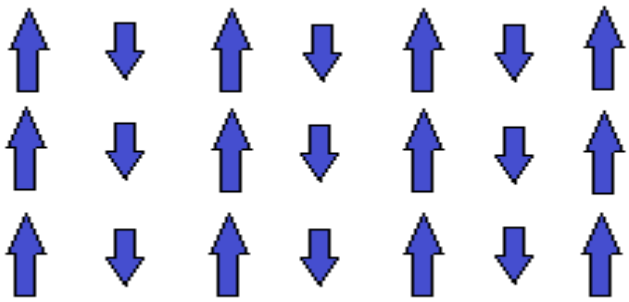

Figure 1.12: difference between ferrimagnetism and anti-ferromagnetic

1.4. Concept of phase transition

1.4.1. Definition

There are specific characteristics that can be observed in a substances state. These include deferent physical forms, such as ice, liquid or solid. Deferent states of matter have different densities, heat capacities and other properties. Differences in the state are visible even with the naked eye and can easily be tested via a magnet or a ruler. By applying high pressures to a sample of ice, several varieties of ice can be obtained. These include amorphous and crystalline varieties of solid water. Different arrangements of atoms, molecules or particles associated with a substance can be observed. This is because different properties of a substance can be seen in different phases of ice. For example, applying higher pressures to water can make several phases of ice that include amorphous and crystalline varieties of water. For some liquids, either an isotropic phase or a liquid crystal phase can be obtained, distinguishable by their optical properties and differing in their molecular orientations, displaying phase transitions or changes of state. Phase transitions occur naturally as water condenses into clouds, or water drops crystallize into ice. They are also observed every day in everyday life, as water evaporates from a moist object. People have used phase transitions for centuries in engineering and industrial

processes. Evaporation of water creates steam that powers turbines, which in turn generates power for electricity generation. Metals can become liquid, and solid and go back to liquid again through metallurgical processes that require physical changes in temperature [16].

1.4.2. Phase transition properties

Water's phase diagram, which is plotted in the Figure (1.13) as pressure versus temperature, demonstrates the plot of pressure and temperature against each other. The lines indicate areas where two phases can exist in equilibrium. This demonstrates that water exists in two phases' liquid and gas at equilibrium. Different states of matter liquid, solid and gas are in equilibrium along a vaporization, fusion and sublimation curve. However, these states of matter can be changed by heating or cooling the system. When it's at a temperature below the critical point, the material is in a vapour phase. The Celsius temperature scale is based on the fact that two pressures determine one temperature. The scale is in thermal equilibrium with two pressure phases [17].

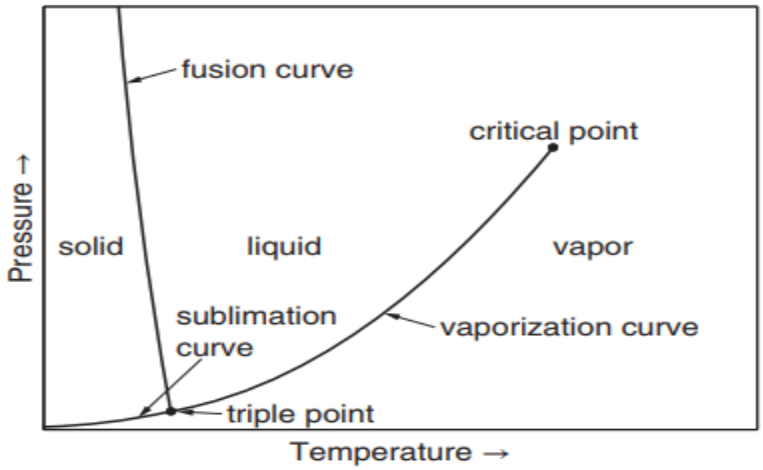

Figure 1.13: Phase diagram of PVT system

The 0°*C* is the temperature at which ice and water reach equilibrium in standard atmosphere (101.325 kPa), and 100°*C*as the temperature at which water vapour (water vapour) and liquid water reach equilibrium at standard atmospheric pressure. These two temperatures called freezing point and vapour point.

An example there is Ferromagnetic-paramagnetic transition when a piece of ferromagnetic material is placed in a magnetic field B, an average magnetization M proportional to B is induced in the material. Then, if we take an axis along B, we can use scalars B and M (assuming they are along the same direction!). The relationship between the applied magnetic field and the resulting magnetization is given by the isothermal magnetic susceptibility, defined by the relationship [18]:

$$\chi_T = \left(\frac{\partial M}{\partial B}\right) \tag{1.15}$$

Note that this is an example of a response function. For fluids, an analogous response function is the isothermal compressibility.

1.5. Classification of phase transitions

Classification of phase transitions is divided into first and second order. First order phase transitions have discontinuous changes in specific heat and other properties. They also have latent heat associated with them, since freezing and melting of water, as well as its evaporation and condensation at lower temperatures, are first order transitions. Other first order phases include temperature changes below the critical point and water classifications. Critical points in a systems second-order phase transition manifest a continuous change in the systems properties. There is no latent heat of transformation during this transition; instead, energy is constantly changing. Systems exhibit strange behaviour at a key moment in their evolution, as their description requires the study of mathematical singularities.

1.5.1. Classification of Ehrenfest (1880 - 1933)

The First classification of general types of phase transitions of matter proposed by Paul Ehrenfest in 1933, at the cross roads of the thermodynamic study of critical phenomena. It arose after the discovery in 1932 of a startling new phase transition in liquid helium, the "lambda transition", when WH Keesom and colleagues in Leiden, the Netherlands, observed an A-shaped "jump" discontinuity in the curve, representing the temperature. The dependence represents the specific heat of helium at a critical value. This apparent jump prompted Ehrenfest to introduce a classification of phase transitions based on jumps in derivatives of free energy functions. AJ Rutgers immediately applied this classification to the study of MelŁstransition from the normal state to the superconducting state. Eduard Justi and Max von Laue were quick to question the possibility of his class of "second-order phase transitions" of which the "lambda transition" was considered a prototype. But CJ. Gorter and H.B.G. Casimir demonstrated their existence in superconductors by means of an "order parameter". Ehrenfests classification was forced to undergo a slow, adaptive evolution in the following decades as a crossroads of research [19].

For a systems energy level to change, it must either increase or decrease in pressure or volume. These changes in state can be measured using the temperature and pressure of the system. The free energy of a system at 0 degrees Celsius is dented by its entropy and temperature, and its Gibbs free energy is determined by its pressure and temperature. If either the temperature or pressure is changed, then the other independent variable needs to be changed as well. This makes thermodynamics a study of energy levels that change due to pressure or volume changes.

This is the study of energy levels that change due to changes in temperature or pressure; this includes calculating the Gibbs free energy. By changing these variables, any other independent variable in thermodynamics can be changed. This allows for people to change any other aspect of thermodynamics, allowing for multiple applications. These applications come in many forms: examining systems with different pressures and temperatures, measuring entropy, and predicting future states based on current states [17].

The relevant thermodynamic potential is the Gibbs free energy when the independent variables are temperature and pressure

$$G = E - TS + PV \tag{1.16}$$

Whereas if they are the temperature and the volume, it is the Helmholtz free energy

$$\mathrm{F} = \mathrm{E} - \mathrm{TS} \tag{1.17}$$

For a simple system, these free energies are differentiated as follows

$$\mathrm{dG} = -\mathrm{SdT} + \mathrm{VdP} \tag{1.18}$$

$$\mathrm{dF} = -\mathrm{SdT} - \mathrm{PdV} \tag{1.19}$$

If the system has a magnetic moment, there is an additional term "-MdH" in the above expression. If the number of particles N is variable, the term " dN" must be added, where " " is the chemical potential. The first derivative gives us the value of a physical property of the system, such as the specific volume

$$\frac{V}{N} = \left(\frac{1}{N}\right)\frac{\partial G}{\partial P} \tag{1.20}$$

The entropy is given by:

$$S = -\frac{\partial G}{\partial T} \tag{1.21}$$

So the magnetic moment is given:

$$M = \frac{\partial G}{\partial H} \tag{1.22}$$

And its second partial derivatives give properties such as specific heat, system compressibility and magnetic susceptibility.

$$C_p = T\frac{\partial S}{\partial T} = -T\frac{\partial^2 S}{T^2} \tag{1.23}$$

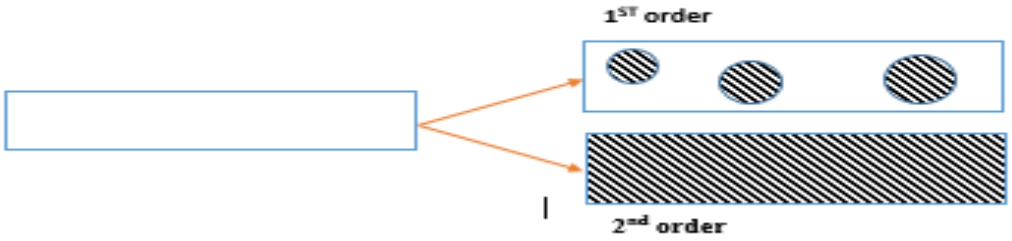

Figure 1.14: Two possibilities of change δG the free energy associated with the phase transition of the 1St and 2Nd order.

When changing the temperature of an environment, a sudden change in energy is impossible. This is because of the conservation of energy. If we consider the free energy per unit volume, g, of a system with a specific number of particles and write G=g.V, only two possibilities exist. A phase change causes a systems properties to change. When this change results from an increase in free energy density, it is referred to as g.G=V.∂g. Alternatively, when it results from a volume increase, it is referred to as ∂V.∂G=g.∂V. Either way, the change causes properties throughout the system to change at once or in different areas of the system to initially only grow ∂V and shrink dg. This can be seen in Fig 1.14. In order to form stable nuclei, or regions large enough to maintain their size, instead of shrinking or expanding, the energy must consist of a negative volume term that is, a volume decrease instead of an increase and the positive surface area are proportional to r3 and r2 respectively. For a spherical nucleus of radius r, this critical dimension r is the dimension at which the volume term is equal to the surface area, so that for $r>r_c$ the growth of the nucleus leads to a reduction in its energy. Because of the need for nucleation, the first phase can coexist with the second phase in a metastable state, even beyond the critical temperature for the phase transition. This is a first order phase transition. The most famous manifestations of this transition are hyperthermia and hypothermia [20].

Both the older phase and the newer phase replace one another across the critical point $\partial G = V \partial g$. While their difference in gaseous properties is slight, the old phase can't persist as a whole across the critical point. Instead, it transforms into two new phases associated with different symmetries. Changes in the systems magnetic properties occur suddenly at some point in the two-phase cycle. This is seen in the paramagnetic and ferromagnetic states of magnetism. Ferromagnetism results from a larger magnetic moment than paramagnetism, so systems with this property have their critical point at one end point of both phases.As suggested by Ehrenfest, phase transitions are classified according to the order of the free energy derivative, which becomes discontinuous because, in modern terms, it is singular at the phase transition temperature [21].

1.5.2. Classification of Landau (1908 - 1968)

L. Landau suggested a specific transition phase classification beyond the continuous category, considering the latter to be a misleading name. He based this on the belief that any transition, even if it doesn't change symmetry of the system, will cause a change in structure [18]

Landau used Polarized Ferromagnetic Paramagnetic Transition to represent the process of magnetization in the space. The direction of ferromagnetism predominates over the isotropic phase. This led to the creation of parameter order. Zero is the smallest magnitude measured in two equal phases. Most often, this is when temperature is at its highest point.

In the classification proposed by Landau, a first-order phase transition translates into a jump in the order parameter (discontinuity) while higher-order transitions (also called continuous) correspond to discontinuities in the derivatives of thermodynamic functions. In the latter case, they can be of the second order if the second derivative is discontinuous, of the third order if it is the third order derivative, etc. These phase transitions are called continuous transitions or critical phenomena.

In a system for which there is a phase transition, there is competition, in the thermodynamic function which characterizes it, between the internal energy which tends to favour order and the entropy which on the contrary favours disorder. If there is no exotic coupling between the degrees of freedom of the system, the disordered phase is generally observed at high temperatures.

1.6. Order parameters

1.6.1. Broken symmetry

Contrary to metaphysical expectations, nature does not always favour the most symmetrical arrangement. Aristotle said planetary orbits had to be circular because they were "perfect" - apparently they weren't [22].

Often, at low temperatures, substances change into phases that do not have the inherent symmetry of the system. The atoms solidify into a lattice, which violates the translation invariance of the Hamiltonian. The atomic spins in ferromagnetic materials are aligned in

specific directions, violating spin invariance. A symmetry is said to be "spontaneously broken" if the Hamiltonian is invariant under a given symmetry operation and the ground state is not invariant. Assume that P is a symmetric operation of the Hamiltonian H constant and $_0$ is the ground state wave function. We have:

$$H\Psi_0 = E_0\Psi_0 \tag{1.24}$$

$$\mathrm{P}^{-1}\,\mathrm{HP} = \mathrm{H} \tag{1.25}$$

That means

$$\mathrm{P}^{-1}\,\mathrm{HP}\Psi_0 = \mathrm{E}_0\Psi_0 \tag{1.26}$$

$$H(P\Psi) = E_0(P\Psi_0) \tag{1.27}$$

If P is a different state from $_0$. It is an equally valid ground state. Therefore, if the symmetry is broken, the ground state must be degenerate. In the breaking of a continuous symmetry, the ground state must be infinitely degenerate. For a Ferro magnet, the total spin of the systems must point along a definite direction, but it can be any direction in space. A consequence of this degeneracy is the existence of spin wave excitations, in which the spin direction varies slightly from point to point in space, as illustrated. In the long wavelength limit, the excitation energy is vanishingly small, because locally the system is in a possible ground state. This is call a "Goldstone mode", the signature of a broken continuous symmetry,

The physical origin of spontaneous magnetization is the attractive force between parallel spins. They prefer to align and rotate as a block. However, this organizational tendency is opposed to random thermal variations, and the balance between these opposing forces determines the average block size at a given temperature. At high temperatures, the bulk sizes are small, and their random spin orientations cancel each other out, leaving no net magnetization. As the temperature is lowered, larger blocks become more stable, and it becomes less common for blocks to change their spin orientation due to thermal motion. This is because changing the spin orientation of a block requires spontaneous coordinated rotation of the individual spins, which is unlikely for bulky blocks. Symmetry breaking occurs because the system remains stuck in a particular configuration for a long period of time. That is, it stems from periodic failures .The competition between spin alignment and thermal motion is reacted in the free energy A=U-TS, where U favors minimization by spin alignment. Instead, S seeks to maximize by randomizing the spin orientation. As I decreases, the alignment force gains support and gains at $T=T_C$, where $UT_CS=0$". The occurrence of spontaneous magnetization leads to a sharp phase transition at the thermodynamic limit. The rotational symmetry is broken

in the low-temperature phase and "recovered" in the high-temperature phase. The subject of this chapter is the phenomenological theory of such phase transitions, usually of second order.

We abstract the concept of an "order parameter" from the spontaneous magnetization, whose appearance below the critical temperature marks a symmetry breaking phase transition.

1.6.2. The ising spin model

In a simple model of ferromagnetism, the Ising spin model, we illustrate spontaneous symmetry breaking. It consists of a lattice of two-valued spins with $s_i = 1$

System	order parameter	Symmetry broken
Ferro-magnet	Magnetization	Rotational Invariance
Antiferro-magnet	Staggered magnetization	Rotational Invariance
Coexisting liquid-gas	Density difference	Spatial homogeneity
Superfluid	Condensate wave function	Global gauge invariance

Tableu 1.2: some examples of ising spin models

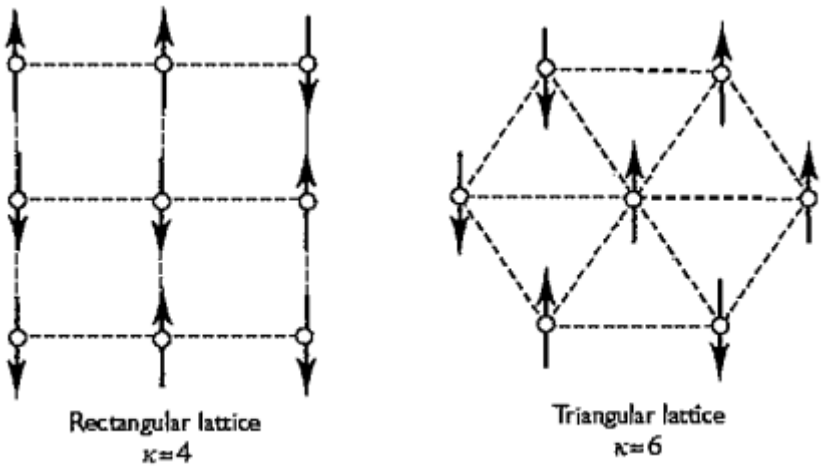

Figure 1.15 two Ising spin model in 2D

In D-dimensional space. The number of nearest neighbours to a given site is denoted by k. A few examples in the 2D space are shown in the figure (1.15). We assume that the physical results are independent of the boundary conditions and that the total number of sites N is large enough. We denote a spin configuration with

$$[S] = [S_1, S_2, \dots, S_3] \tag{1.28}$$

And the energy with

$$E[S] = -\varepsilon \sum_{ij} S_i S_j - h \sum_i S_i \tag{1.29}$$

Where <*ij*> denotes a pair of nearest neighbours and h is a uniform external magnetic field. The magnetic moment of a spin is unity in our units. The constant is positive for a ferromagnet and negative for an antiferromagnet. We assume ε>0. The canonical ensemble mean of the total spin is the magnetization

$$M(h) = \frac{\sum_i S e^{(-\beta E_{[S]})} \sum_i s_i}{\sum_i e^{(-\beta E_{[S]})}} \tag{1.30}$$

With $\beta = 1/k_B T$, we call this the order parameter.

When h = 0, there is up-down invariance: E[*S*] = E[*S*]. Therefore, spontaneous magnetization seems impossible, because changing the summation variable from [*S*]to [-*S*] we find that M(0)=-M(0), so M(0)=0. The solution to the paradox lies in an argument we made earlier: in the limit N→∞, at sufficiently low temperatures, the system cannot sample all available configurations in finite time. Mathematically, this can be expressed by the fact that the limits of h→0 and N→∞ do not oscillate at sufficiently low temperatures:

$$\lim_{N\to\infty} \lim_{h\to 0} M(h) = 0 \tag{1.31}$$

And the mean field approximation consists of replacing each nearest-neighbour spin with the average spin per particle, which is given by

$$m(h) = \frac{M(h)}{N} \tag{1.32}$$

Hence, the sum of the nearest neighbour spins gives a factor *m*:

$$\mathrm{W(Si)} = -[\,\mathrm{h} + \in \mathrm{km}]S_i \tag{1.33}$$

An effective magnetic field is applied to the spin s

$$H_{eff} = h + m \tag{1.34}$$

The internal energy of the particle in the mean-field approximation is

$$U = -Mh_{eff} = -Nm\left(h + KT_C m\frac{\partial m}{\partial T}\right) \tag{1.35}$$

The specific heat of a constant external feld at the point h = 0 is given by

$$\mathrm{C} = \frac{1}{\mathrm{N}}\left[\frac{\partial \mathrm{U}}{\partial \mathrm{T}}\right]_{\mathrm{h}=0} = -2\mathrm{kT_C\,m}\,\frac{\partial \mathrm{m}}{\partial \mathrm{T}} \tag{1.36}$$

The mean field approximation is incorrect in detail. It predicts a phase transition independent of D, but in fact there is no phase transition for D = 1. Nonetheless, it illustrates in a simple way how spontaneous magnetization can occur suddenly in theories that deal only with continuous functions.

1.6.3. Critical exponents

During phase transitions, systems move past a point of transition. This means they show unique physical characteristics nearby their boundaries. Calculating power laws at this point helps determine the type of critical transition the system will undergo. When people calculate power laws, they use critical exponents that determine specific properties of the system near its boundary. We determine a magnetic systems natural order parameter; this is the natural candidate for "m" in the equation. Its corresponding ordering field "h" is the quantity $B=Kt_c$. In terms of this parameter," h" tends to m_0, which is the limiting value for $T \approx T_c$. However," h" has a property that it cannot go past 0 for $T < T_c$; the value of T_C depends on the details of the atomic or molecules interactions of the system and hence will vary widely from one system to another. Any macroscopic variable can be written as F (T) with the reduced temperature θ_C expressed by:

$$\theta_c = \frac{T - T_c}{T_c} \tag{1.37}$$

Then a critical exponent s for $\theta_C \approx 0$ such that $T \approx T_C$ can be determined by:

$$F(\theta_c) = A\theta_c^{-s} \tag{1.38}$$

Where A = constant. Note that there are two broad situations, which depend only on the sign of the critical exponent, as below:

1. Positive critical exponent s, F (θ_C) diverges as $T \rightarrow T_C$.
2. Negative critical exponent s, $F(\theta_C) \rightarrow 0$ as $T \rightarrow T_C$

In fact, it can be expected that F will behave analytically far away from the fixed point.

With this in mind, we can rewrite it with a wider range of validity, as follows:

$$F(\theta_c) = A\theta_C^{-S}(1 + B\theta_C^{Y} + \cdots) \tag{1.39}$$

Where y >0 in the case of large θ_C and B is a constant. In more formal terms, the critical exponent s of F (θ_C) is defined as follows:

$$S = \lim_{\theta \to 0} \frac{InF(\theta_c)}{In\theta_c} \tag{1.40}$$

spesific heat (for B = 0)	$C=\|t\|^{\alpha}$
order parameter	$M=(-t)^{\beta}$
susceptibility (B = 0)	$\chi=\|t\|^{-\delta}$
critical isoterm (t = 0, B ! 0)	$H=\|M\|^{\delta}$
correlation function	$G(r)=\| r \|^{d\,2+\eta}$
correlation length	$\mathfrak{E}=\|t\|^{\nu}$

Tableau 1.2: dentition of critical exponent

In addition to this, we should note the commonality of critical thinkers. Most share a common understanding due to the abstract nature of their Hamiltonian and atomic interactions.

1.6.4. Universality

We cannot resolve spatial structures smaller than E because the field organizes into uniform blocks of about that size. As we approach the critical point, E increases and we lose resolution. At the critical point, when E diverges, we don't see any detail at all. Only global properties such as spatial dimensions or number of degrees of freedom distinguish one system from another. Thus, systems at a critical point belong to the pervasive category characterized by a criticality exponent.

Imagine you're blindfolded in a room that can only be probed with a very long pole. Whether the room has an ID, 2D or 3D by trying to move a pole, but you can hardly learn anything else. Likewise, if you put on very dark glasses, you'd conclude that all places on Earth are equal and characterized by a 24- hour light-dark cycle. To experience new things, you have to go to Mars.

Chapter 2

2.1. Introduction

Lattice spin models currently play an important role in the description of different metals and in deducing their different magnetic characteristics as a function of the modification of some external parameters. This cannot be without the use of various methods of statistical mechanics. Approximate methods such as mean field and effective field ones and exact methods such as the Monte Carlo and the transfer matrix ones are increasingly used to study different physical phenomena.

2.2. Spin models

2.2.1 Generals information

Describing phase transitions theoretically is a highly complex task, and only a few models can be analysed within the framework of statistical mechanics. One such model is the Lenz model (1920), which was later elaborated on in detail by his student, Ising (1925). This simple model of statistical thermodynamics plays a critical role in our understanding of phase transitions and critical phenomena and has allowed for the development of statistical mechanics methods in the field of physics [23]. To better structure the idea, we use the term "Hamiltonian", which refers to the energy of the system. It's important to note that for quantum systems, the Hamiltonian is an operator, and the energy is its eigenvalue [24].

2.2.2. Notion of spin

Atomic physics shows us that in each layer of the atom, electrons are specified in terms of their orbital angular momentum. So that as each electron moves, it carries with it a half quantum of the so-called spin or intrinsic angular momentum and an associated magnetic moment. Although spin is a new degree of freedom characterising most quantum mechanical particles, it appears that spin must be thought of as an intrinsic angular momentum of a particle. Moreover, spin is dissociated from all other degrees of freedom of a particle, so that the spin operator commutes with all other dynamical quantities [25]. It has only two directions with respect to a given orientation, parallel or antiparallel [26]. For our purposes, the behaviour of spins in different lattice structures has been a magnetic phenomenon. Moreover, the characteristics of magnetic materials and their technological applications such as thermomagnetic recording media [27], and micro-electromechanical systems; are characterised by the phenomenon of mixed spins which are well defined in the Ising model approach [29].

2.2.3. Lattice spin models

2.2.3.1. Ising model

In the previous chapter, we explored the phenomenology of phase transitions, and now we turn our attention to the Ising model wich is significant as it is the simplest statistical model that exhibits a phase transition. There are two primary reasons for studying this model. Firstly, to simplify the spin nature, making it possible to solve the system exactly, and secondly, to compare it with other models as it is realistic enough. The Ising model was first introduced by

Wilhelm Lenz in 1920, and since then, numerous scientists have contributed to understanding its mathematical properties. Ernst Ising, made the first theoretical discoveries in 1925[29]. In his doctoral studies, he presented a brief paper demonstrating the absence of phase transition in the one-dimensional case. From that point on, the model has been named in the literature as the Ising model. Lenz and Ising endeavoured to replicate the features of paramagnetic and ferromagnetic solids through their model, which employed statistical mechanics to micro-magnetics [30].

When defining a structure, it's easy to say that each node represents an element. However, for a regular space network, each node is linked to a variable with one of two values: +1 or -1. A configuration of the lattice is a particular set of values of all the spins; if there are N nodes, there will be 2N different configurations; typically the two-valued variable is denoted by the spin I associated with node I of the lattice [31]. We assume that the molecules exert only short-lived forces on each other; in fact, we acknowledge that the only factor that affects the interaction energy is the arrangement of the molecules [32]. For a mathematical study of any physical system, it is necessary to introduce the Hamiltonian which is the total energy of a system in mathematical physics, and its dynamics are determined by it. So, we can calculate all its characteristics from it based on modifications made on external parameters [33].

For each configuration $\sigma = \sigma_1 \ldots \sigma_N$, we have: under the assumption that only short-range interactions, "closer-to-neighbour" interactions, and interactions of lattice sites with an "external field" contribute to the system's energy level, the Hamiltonian is given as follows:

$$H = -\sum_{\langle i,j \rangle} J\sigma_i \sigma_j - \sum_i H\sigma_i \tag{2.1}$$

The parameters J and H are the "energies" associated with interactions with the external field in the case of a material ferromagnetic. The first sum includes all pairs of nearest neighbours in the network, while the second sum includes all sites in the network. The J character then reflects the presence of an "external magnetic field," which tends to orient the magnetic moments in the field's direction, whereas random thermal agitation negates much of the magnetic field's effect [34].

The figure below illustrates this pattern and depicts a pair of adjacent spins plotted on a square grid. J is a constant of coupling or interaction: if J is negative, this indicates the presence of a ferromagnetic interaction and in the opposite case if J is positive, one will have the presence of an anti-ferromagnetic interaction [35].

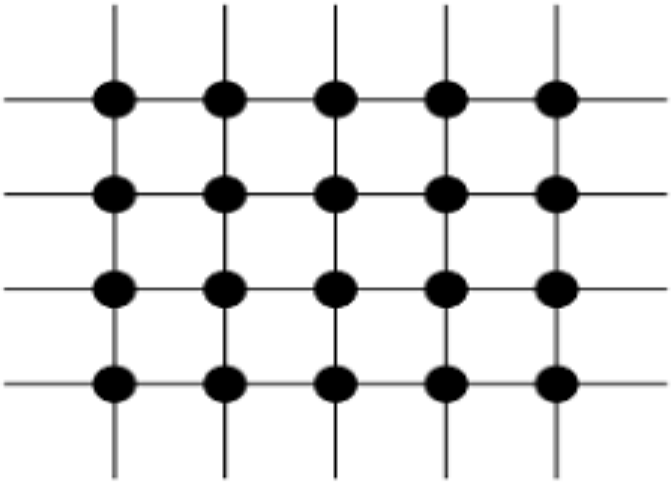

Figure 2.1: Square lattice with different nearest neighbour sites ij

Onsager's ground-breaking research paper provided the first-ever precise solution to a two-dimensional ferromagnetic Ising model in a zero magnetic field on the rectangular lattice. This model displays a phase transition. Onsager's original derivation is known for its mathematical complexity; however, since then, multiple simpler solutions to the problem have emerged [35]. Among these, Schultz and others, calculation stand out as an excellent example of an exact statistical physics calculation. While most of the book focuses on approximation techniques like as mean-field theory and approximate renormalization group calculations [36].

2.2.3.2. Potts model

Potts' statistical mechanical models of magnetism are highly similar to permeability and were initially introduced by Potts in 1952. These models serve as a generalization of the simple model of ferromagnetism presented by Ising in 1925. For the sake of precision, let's consider a lattice that is locally square. Each lattice location i can be associated with a pair of nearest neighbour sites S_i, and a variable or spin can be assigned to each of these locations. This variable represents the local microscopic state of a physical system and is relevant in a variety of cases [37]. Therefore, Potts' models hold significance in their own right. This system is determined by two parameters. The first is an inverse temperature parameter, which is similar to percolation's density parameter p. The second parameter, q, corresponds to the number of states available at each site. If q=1, the model is equivalent to percolation, and if q=2, it is equivalent to calculating Ising magnetization. For q=3, 4 Potts models exhibit second-order transitions in two dimensions, while for q>5, these models have first-order transitions in all dimensions [38].

The Hamiltonian for this system is as follows:

$$H = -J\sum_{\langle i,j\rangle}\delta\left(\sigma_i,\sigma_j\right) \quad (2.2)$$

This is a statistical model where at each point in a network of q discrete values σ_i=1 , 2 ,..., q there is a variable called it. In this model, two spins that are close to each other have an interaction energy that is given by $-J\,\delta(\sigma_i,\sigma_j)$ [37].

2.2.3.3. Blume-Emery-Griffiths model BEG

2.2.3.3.1. Definition

For studying physicochemical systems, the Blume-Emery-Griffiths model BEG has been extensively employed over recent decades. Its primary purpose was to explain the He^3-He^4 binary mixture. Due to its immense success in qualitatively describing the system's behaviour, it gained popularity. The model accurately predicts second and first-order transitions, with the latter responsible for phase separation and the emergence of a tricritical point.

With the BEG model, binary mixtures containing a magnetic or superfluid degree of freedom can be effectively modelled. To model the He^3 - He^4 mixture, Blume, Emery, and Griffiths employed a lattice spin system that can result in a ferromagnetic order. While this order is interpreted as superfluidity, its identification is purely based on a phenomenological analysis.[39].

2.2.3.3.2. Theoretical study of the BEG model

In 1951, Heer and Daunt were the first to study liquid helium mixtures on the basis of theoretical models. These mixtures were considered to be isotopic mixtures in 1954 by Prigorineand others. Using known experimental data, they concluded that phase separation must occur at 1°K.

In 1960, Cohen and Van Leeuwen studied a binary hard-sphere mixture of fermions and bosons as a model for a ^{3}He-^{4}He liquid mixture and obtained a phase diagram similar to that of a helium mixture [40].

In 1966 Bardeen Baym and Pines proposed a semi-phenomenological model around T instead of a logical model around T = 0°K. The model takes into account the interactions between fermions. The phase diagram obtained is consistent with that of helium at temperatures below 0.4°K.

An Ising spin-1 model was not proposed until 1972 by Blume, Emery and Griffiths. Using the mean-field approximation, they obtained a phase diagram qualitatively similar to that of helium mixtures, with one exception, namely that the phase separation is complete at T = 0K. By

varying the nature and length of the interactions between the spins, they were able to obtain other phase diagrams in which the tricritical points do not appear.

The Hamiltonian that describes these systems is written, in its most general form, as follows:

$$\mathcal{H} = -h\sum_{J=1}^{N} S_J + \Delta\sum_{J=1}^{N} S_J^2 - J\sum_{\langle i,j\rangle} S_i\,S_j - H_3\sum_{\langle i,j\rangle} S_i\,Sj\left(S_i + S_j\right) - k\sum_{\langle i,j\rangle} S_i^2 S_j^2 \quad (2.3)$$

Where each of the spins can take on the values 1, 0, and -1. H and Δ are the external magnetic field and crystal field respectively. J and K are bilinear and biquadratic exchange interactions and H_3 is a third-order perturbation.

Our definition of the order parameters of the model is as below:

a- Magnetisation m

The magnetisation m concerning a site in the lattice is given by

$$m = \langle S_{\mathrm{i}}\rangle = \frac{\sum_S S_{\mathrm{i}} e^{(-\beta H)}}{\sum_S e^{(-\beta H)}} \quad (2.4)$$

This is summed over all the configurations used in the system.

b- Quadruple order q

Denotes the average value of the square of the spin, given as

$$q = \langle S_i^2\rangle = \frac{\sum_s S_i^2\, e^{(-\beta H)}}{\sum_S e^{(-\beta H)}} \quad (2.5)$$

C- Moment octupolaire r

$$r = \langle S_i^3\rangle = \frac{\sum_S S_i^3 e^{(-\beta H)}}{\sum_S e^{(-\beta H)}} \quad (2.6)$$

2.2.4. Blume Capel model BC

Blume and Capel, two physicists, introduced the BC model as a variant of the BEG model without quadrupole interaction [41]. This model served as an ideal tool to study tricritical phenomena and was initially designed for spin-1 to analyse magnetic systems, as well as to

delineate the phase separation in He3-He4 mixtures. These researchers named this model after themselves, having proposed the idea separately [42].

Thus, various statistical mechanics techniques, including Mean-Field Approximation (MFA), Monte Carlo (MC) Simulation, Transfer Matrix Calculations (TMC)[43],[44] and Coupling Constant Approximation, employed this model [45].

Extending the interaction to neighbours other than the nearest neighbour is of great interest for theoretical reasons. In this context, we can cite previous work that introduced a second-neighbour interaction that creates a kind of competition between the two types of coupling. Bedahdeh and others, investigated the anti-ferromagnetism of the 48-spin-1-BC model considering these two interactions and the field state results indicated the emergence of new frustrated phases in addition to those found in By Buzzing et al. Another work some ten years later can also be mentioned: Dias and others,two exchange interactions are considered to investigate the BC spin-1 model on simple cubic lattices.

$$\mathcal{H} = -J_1 \sum_{\langle i,j \rangle} S_i S_j - J_2 \sum_{\langle i,j \rangle} S_i S_j + \sum_i s_i^2 - H \sum_i S_i \tag{2.7}$$

2.2.3.4. Heisenberg model

In 1928, the Heisenberg model was first introduced, providing a way to describe the properties of certain magnetic insulators like EuS. It presents a microscopic Hamiltonian that accounts for the exchange interaction responsible for ferromagnetism. Nonetheless, the model assumes spin isotropy and lacks the possibility of non-localised spins. In contrast to the Ising model, the Heisenberg model does not switch spin operators, making it more quantum-like and harder to approach analytically or numerically. Though one-dimensional quantum models have exact results, transposing quantum models to classical spin systems in higher dimensions is possible, as is the case for two-dimensional classical models [46].

$$H = -J \sum_{i,j} S_i \, S_j - H \sum_i S_i \tag{2.8}$$

While it is possible to continuously vary the anisotropy and study the resulting phase transitions, spin is quantized. It is speculated and generally accepted that integer and half-integer spin Heisenberg models behave very differently. Therefore, it is of particular interest to devise methods that allow the continuous connection of models with different spin values [47].

2.2.3.5. Ashkin-Teller model ATM

1. Generality

Ashkin-Teller model ATM comprises two layers of Ising spins that interconnect via a four-spin system, producing a two-dimensional configuration [48]. Within each model, the closest neighbour Ising spins interact twice, their coupling determined by the four-spin interaction parameter. Essentially, the Ashkin-Teller model is the union of two Ising models [49], each with their distinct coupling constants, K_1 and K_2. Via duality transformation, the Ashkin Teller model can be reconstituted as an 8 spin model. In the absence of K_3, the Ising models are uncorrelated, and two unique transitions occur [50]. However, the effect of K_3 remained unknown until Lin and Wu utilized an aggregation of available data and a continuity analysis to confirm the occurrence of two-phase transitions in the Ashkin-Teller model. Following their initial work, Ashkin and Teller proceeded to create an intriguing model [51].

The study of statistical mechanics was simplified by Ising systems, paving the way for the comprehension of cooperative phenomena of quaternary alloys in a lattice. The Hamiltonian, used to describe magnetic systems, was made adaptable to the model. By superimposing two Ising models, the Ashkin-Teller model was established, consisting of spin variables S_i and σ_i residing on a lattice's sites. Exchange interactions between adjacent variable spins were observed in every Ising model J_{ij}, coupled by four spin interactions with a coupling K_{ij}. Nearest neighbour spins were calculated in the sums [52].

$$H = -J \sum_{\langle i,j \rangle} \vec{S}_i \vec{S}_j - \sum_i \vec{S}_i \tag{2.9}$$

In 1941, Kramers-Wannier observed a critical point for a special case of the Ashkin-Teller model in which three of the four components are degraded [53]. Their assumptions extend to the Ashkin-Teller model shown by Fan (1972) [54] and lean towards the model of Wegner (1972), who generally proves that arguments do not exist at critical points. Prove that the argument does not exist at the critical point [55]. It is therefore interesting to study the transition problem in this model in detail. Wagner also showed that the Ashkin-Teller model is equivalent to the alternative eight-node model, but it was not exactly solved. A single critical line in the phase diagram of the isotropic Ashkin-Teller model is as accurate as possible because of the duality relationship discovered by Fan [56].

One of the most interesting key properties of the model is the non-generality of the key behaviour on the self-doubling line, where the key exponent is constantly evolving. On the other hand, 3D models have been shown to have richer phase diagrams than 2D ATM models. There are first-order phase transitions and continuous phase transitions. There are even XY-type transitions and Heisenberg-type multiple critical points [57].

Ditzian and others conducted of the standard (3D) AT model and discovered a phase diagram that differed greatly from that of the (2D) groups. Unlike the d=2 groups, the d=3 groups demonstrated a new phase where the system spontaneously broke its natural symmetry between

two Ising spins. The renormalisation group's concepts provided a comprehensive explanation for the observed series of continuous transitions [58]. Arnold and Zhang achieved more precise results through numerical simulations of the Ashkin-Teller model, which supported theoretical techniques for studying very weak first-order phase transitions in three dimensions. [59] In this case, the first-order transition's universal quantities characterise it. Using Monte Carlo simulation to measure the relative discontinuity of specific heat, correlation length, and susceptibility across the transition, Zbigniew Wojtkowiak and colleagues studied a cluster Monte Carlo method that adapts to first and second-order phase transitions in the 3D Ashkin-Teller model. Surprisingly, they found no observable critical slowing or the presence of metastable or unstable states on the values of the thermodynamic quantities. Moreover, they verified the suitability of their cluster algorithm for continuous and first-order phase transitions in the 3D AT model when using the Metropolis algorithm [60].

In collaboration with S. Bekhechi and several others, Badehdah delved into the anisotropic spin-1/2 AT model. Using the transfer matrix method, they uncovered additional partially ordered phases. Their findings, based on precise numerical computations, revealed that all transitions operate under the Ising universality concept, with the exception of the B4 multicritical point on the phase diagram, which stands out as non-universal. Additionally, exponent calculations lent weight to their assertions [61]. While examining the AshkinTeller spin-1 model for unrelated research, they discovered intriguing phase diagrams with a plethora of first and second-order phase transitions in parameter space (K_4/K_2, D/K_2, T/K_2). Further still, specific values of (K_4/K_2) and (D/K_2) highlighted partially ordered phases PO_1 and PO_2. The critical exponent revealed a line of critical points exclusive to the four-state Potts model when the anisotropy was within a specific range. As for the spin-1/2 ATM, a lower (D/K2) categorized the model as an Isingtricritical universality class [62].

2. Applications of the Ashkin-Teller model

The Ashkin-Teller model was devised after observing a selenium compound being absorbed onto a Ni surface. By scrutinizing sub-monolayers of Ni (100), they detected p (2x2), c(2x2), and disordered phases, while pinpointing their respective boundaries. Through symmetry arguments, the universality class of the phase diagram was assigned to the Ashkin-Teller model [63], predicting critical behaviour near its phase boundaries and at the multicritical point of convergence. A DNA elastic response, characterized by the main stack interaction, yielded a corresponding phase diagram. In particular, stretching and twisting induced a transition from the B model state to the S state, with the DNA's elastic response presented in a standardized morphology [64].

In addition, the model requires the investigation of the thermodynamic properties of the superconducting capsule (CuO_2 chip), assuming a critical region near its transition, after performing large-scale Monte Carlo simulations on the generalised (2D)Ashkin-Teller model to determine the properties of the thermodynamic calculations. The Ashkin-Teller model contains a pair of Ising loops at each position, which interacts with neighbouring loops through two- and four-loop interactions. The model describes the interaction between the orbital current loops in TC-treated CuO_2 wafers arranged with modulated magnetisation in each unit cell in the unknown region of the first phase diagram. The low-temperature T depends on the doping. However, it is important that the specific heat does not change. This brings the behaviour of the model into an agreement with experimental results in underdopedcuprates [65].

Furthermore, oxygen estimates can also be fitted to a (2D) Ashkin-Teller model in $YBa_2Cu_3O_z$ for different stable configurations determined by Landau-Lifshitz theory and Monte Carlo simulations. A correct Landau-Ginzburg-Wilson-Hamilton analysis shows that critical behaviour is consistent with ranking. The prevalence categories show that key behaviours fit the Ashkin-Teller model [66].

3. Theoretical and numerical methods to ATM

The critical and magnetic properties of the Ashkin-Teller model have been extensively studied in the literature, although the Ashkin-Teller model presents a complex and interesting phase diagram due to the presence of triple critical points and lower-order phase transitions. The properties of the Ashkin-Teller model have been studied using various applied theoretical and numerical methods, including Monte Carlo simulations, which are relevant to the topic of the thesis and are discussed in the Applications section of the next chapter (Mean field approximation [65] and Correlated effective mean field method [66]). Matrix transfer field method [67] and renormalisation group theory [68].

2.3. Usual methods in statistical mechanics

2.3.1. Approximate methods

2.3.1.1. Mean field approximation

Methods that are not precise or accurate, are referred to as approximate methods. These theories are typically used to describe most transitions, often utilizing the molecular field method. The mean field approximation, initially designed for studying interacting body systems, replaces the problem of interacting spins with one concerning independent spins residing in an average field produced by all other spins. In this section, we explore the Ising model's mean-field approximation, which is rooted in the notion that each spin Si feels a typical influence exerted by surrounding spins. For spin 'i', the coupling terms of the form S_iS_j will be substituted with $S_i\langle S_j\rangle$, and it is assumed that the spin average is uniform throughout the material, represented by $\langle S_j\rangle = \Phi_j = \Phi$ [69].

The mean field approximation consists in taking a single spin Si and calculating its energy by replacing all other spins with their mean value $\langle S_j\rangle$. The Hamiltonian including the external magnetic field for the Ising model is:

$$H = -J\sum_{\langle i,j\rangle} S_iS_j - \mu h\sum_i S_i \qquad (2.10)$$

With J coupling constant, h external magnetic field and μ spin magnetic moment. In the mean-field approximation, the spin energy S_i is given by

$$E_i = -JS_i \sum_j \langle S_j \rangle - \mu h S_i \tag{2.11}$$

The site energy has two values E_{i+} and E_{i-}, depending on whether the spin is up (+1) or down (-1):

$$E_{i+} = -J \sum_J \langle S_J \rangle - \mu h = -zJM - \mu h \tag{2.12}$$

And

$$E_{i-} = J \sum_j \langle S_j \rangle + \mu h = zJM + \mu h \tag{2.13}$$

Where M is the average S_j and z is the nearest neighbour. The average Si is expressed by the Boltzmann constant k_B and the temperature T as follows:

$$\langle S_i \rangle = \tan h \left(\frac{zJM + \mu h}{K_B T} \right) \tag{2.14}$$

When there is no external field, the mean field approximation anticipates a phase shift. This shift entails the order parameter's termination above a critical temperature, Tc, resulting in the separation of two phases. A low-temperature phase, exhibiting spontaneous magnetisation, is juxtaposed with a high-temperature phase that does not. Studying the thermodynamic observables' asymptotic behaviour, we must focus on events surrounding the transition. As T approaches T_c, the order parameter Φ becomes uniform and approaches zero. Therefore, we can develop various properties in proximity to the transition, as F tends to zero. One such property, the free energy, can be expressed as:

$$W(T,\Phi) = N\left(w(T,0) + \frac{1}{2}r(T)\Phi^2 + u(T)\Phi^4\right) \quad (2.15)$$

Where W (T, 0), r (T) and u (T) are given by:

$$w(T,0) = -\mathrm{KT}\ln(2) \quad (2.16)$$

$$r(T) = \frac{T_C}{T}(T - T_C) \quad (2.17)$$

$$u(T) = K\frac{T_C}{T} \quad (2.18)$$

When the parameter r(T), which is a function of T-T_c, is positive (T>Tc), the curve W(T, F) has only one minimum at Φ = 0. Conversely, when r(T) is negative (T<Tc), two stable states emerge. This finding is significant because the shape of the free energy, which discloses a phase transition, displays a profound reliance on the sign of the parameter in the vicinity of the critical point.

When compared to exact theories and direct experience, the mean-field theory may be deemed relatively straightforward. It serves as a qualitative explanation for the Ising model's phase transition but falls short of precision. Empirically, various thermodynamic observables display power law behaviour close to critical transitions. Notably, magnetisation and susceptibility exhibit the following trends:

$$\Phi \approx (T - T_C)^{\beta} \quad (2.19)$$

$$\chi = |T - T_C|^{-\gamma} \quad (2.20)$$

The numbers β and γ are called critical exponents.

When comparing the outcome of experiments or exact theories, fascinating observations can be made. In the case of a D=1 system (a chain of spins), the mean field approximation fails miserably, predicting a phase transition that doesn't exist (transfer matrix method) for a chain of spins. The critical temperature for the 1D Ising model is shown to be zero. However, for D=2, there is a phase transition at kT_C=2.27J, and the critical exponents are β=0.125 and γ=1.75, which are significantly different from mean-field values. In the case of a cubic lattice with z=2D

neighbours, the mean-field theory gives a critical temperature of $kT_C=4J$, which is an error of 76%. As the dimension of space increases, the accuracy of mean-field results improves, and they become precise in infinite dimensions [69].

2.3.1.2. Weiss Mean Field Method

Magnetic domain theory was developed by French physicist Pierre-Ernest Weiss, who proposed in 1906 that magnetic domains exist in ferromagnetic materials. He proposed to align a large number of atomic magnetic moments (approximately 10^{12} to 10^{18}) in parallel. The alignment direction of the domains varies more or less ranomly from domain to domain, although certain crystallographic axes, called asy axes, are favoured by the magnetic moment. Weiss still needs to explain why the magnetic moments of atoms in ferromagnetic materials align spontaneously. He presented his theoretical concept called the Mean Field Theory, which suggests that a given magnetic moment in a material is subjected to a strong magnetic field caused by the magnetization of its neighbours. Initially, his theory proposed that the average field was proportional to the material's magnetization, represented by $He= \alpha.M$, where α is the constant of the mean field. However, this approach is not suitable for ferromagnetic materials due to the variation in magnetization from one domain to another. In such cases, the interaction field becomes $He= \alpha.Ms$, where M_S represents the saturation magnetization at 0 K.

In the later years, the field of quantum physics facilitated an understanding of the microscopic roots of the average field (or Weiss field). The exchange interaction between local spins promotes a parallel alignment (in ferromagnetic materials) or an anti-parallel alignment (in anti-ferromagnetic materials) of neighbouring magnetic moments.

2.3.1.3. Correlated effective mean field method

The Honmura and Kaneyoshi duo created the effective field method, which was further refined by Boccara. Unlike the mean field, it delivers superior qualitative and quantitative outcomes while remaining easy to use. However, the method is only effective for systems that employ discrete variables to depict the disorder. The process involves selecting a central spin and computing its average value while keeping all other spins in the lattice constant. The resultant equation of state derived from averaging all configurations allows for the determination of the transition temperature and other system properties.

The approach of utilizing a differential operator:

$$H = -\frac{1}{2}\sum_{i,j} J_{i,j}\mu_i\,\mu_j - h\sum_i \mu_i \qquad (2.21)$$

The Hamiltonian of the Ising model is defined by the presence of an external magnetic field h.

Where μ_i is a dynamic variable that can take two values ± 1, and $J_{i\,j}$ is the exchange interaction between site i and site j.

The order parameter is determined by m = h<μ_i>.In the ordered phase m≠0, while than disordered phase m = 0. The average spin value is given by:

$$\langle m_i \rangle = \frac{1}{Z} Tr \mu_i e^{-\beta H} \tag{2.22}$$

With the Z splitting function:

$$Z = Tr e^{-\beta H} \tag{2.23}$$

$\beta = 1/K_B T$, K_B is Boltzmann's constant

T is the absolute temperature. The Hamiltonian of the equation is expressed as the sum of:

$$H = H_i + H' \tag{2.24}$$

Where the first part H_i includes all contributions associated with the site, while the second part H' does not depend on position i. so,

$$H_i = -\mu_i E_i \tag{2.25}$$

Let E_i be an operator denoting a local field on site i which takes the form:

$$E_i = \sum_{i,j} J_{ij} \mu_j + h \tag{2.26}$$

An approximation of the effective correlated field considers that the central spin μ_i is linked to the nearest neighbour $\mu_i+\delta$ by:

$$\mu_{i+\delta} = h\mu_i + \delta_i + \lambda(\mu_i - h\langle \mu_i \rangle) \tag{2.27}$$

Where λ is a temperature-dependent parameter. After some transformations for h =0 we will have:

$$H = -\sum_i H_i^{eff} \mu_i + cst \tag{2.28}$$

We have also

$$H_i^{eff} = J\sum_j \langle \mu_j \rangle - \lambda J_z \langle \mu_i \rangle \quad (2.29)$$

2.3.2. Exact methods

2.3.2.1. Monte- Carlo method

This is one of the precise algorithmic methods for calculating approximate numerical values using stochastic processes and probabilistic techniques. The name of these methods, referring to the game of chance played in Monte Carlo, was invented by Nicholas Metropolis [70] in 1947 and first published in 1949 in an article co-authored by Stanislaw with the Ulam newspaper and published in 1949 in article. In statistical mechanics, we start with the mean of an observable A for the Boltzmann distribution calculated as follows:

$$\langle A \rangle = \sum_l p_l^{eq} A_l \quad (2.30)$$

Where p_l^{eq} the equilibrium probability distribution is in state l, A_l is the value of A in this state, and l is the system's state:

$$P_l^{eq} = \frac{e^{-\beta E_l}}{\sum_m e^{-\beta E_m}} \quad (2.31)$$

With E_l the energy of state l and $\beta = 1\backslash k_\beta T$ the constant of Boltzman

Typically, the quantity of states is incredibly vast, making summation impractical when considering the thermodynamic limit ($N\rightarrow\infty$). To overcome this challenge, Monte Carlo simulations enable the study of numerous particles by sampling states generated via iterative procedures. Rather than summing over all states in equation (2-1), a subset is used to obtain an estimated mean value, albeit with statistical errors. Binder (1984) provides the following formula for this estimated value:

$$\langle A \rangle_{est.} = \frac{1}{T_0}\sum_{t=1}^{t_0} A(t) \quad (2.32)$$

Where "t" refers to a configuration generated by our algorithm. "A (t)" represents the value of A at time "t", whereas "t_0" denotes the number of measurements taken.

In practical terms, Monte-Carlo simulations are numerical experiments where random visits to states in the phase space occur. Starting from an initial configuration φ, a random configuration φ' is generated. The latter is accepted with a transition probability ω (φ → φ'), which is dependent on the energy variation ΔE involved.

$$\omega(\varphi \to \varphi) = \begin{cases} \exp(-\beta \Delta E), & si\ \Delta E \geq 0 \\ 1, & Si\ \Delta E \leq 0 \end{cases} \tag{2.33}$$

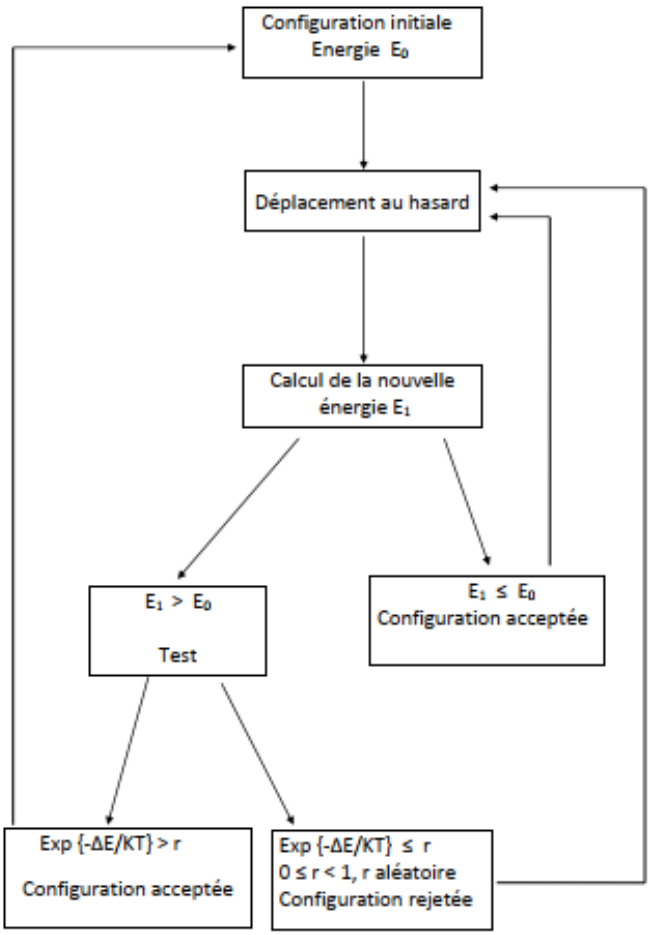

Figure 2.2: Diagram of the standard Monte-Carlo algorithm

The standard Monte-Carlo simulation programme follows a structure consisting of three main steps, as shown in Figure (2.28). In practice, a square grid of L × L is considered, consisting of L^2 sites, where L is the size of the network. The Metropolis algorithm is applied to the model as follows:

We start from the initial configuration, after which a site on the spin network is randomly selected and the energy difference between the two configurations is calculated.

If the difference is zero or negative, the selected spin randomly evolves into one of the other possible states. If the difference is positive, the previous configuration is retained for another sequence.

1. Metropolis Monte Carlo algorithm

In 1953, Nicholas Metropolis proposed an algorithm that would revolutionize the field of computational physics and chemistry. The Metropolis algorithm is a computational method used for generating random samples from complex probability distributions. It is commonly used in Monte Carlo simulations, which involve performing probabilistic calculations to model complex systems. Metropolis' algorithm uses a set of random numbers and a cost function to evaluate the probability of accepting or rejecting a proposed state. This algorithm is widely used in various fields, including statistical physics, biology, and computer science. Metropolis' algorithm has since been developed and improved upon by numerous researchers, and its impact on the field of computational sciences has been significant, its main use is to produce a Markov chain via the algorithm, with the members of the limiting distribution of the chain being the target density $\pi(x)$. The name "Monte Carlo" is derived from the algorithm's dependence on random numbers. This approach allows the estimation of averages of physical quantities using the Gibbs formulation of statistical mechanics expressed as multidimensional integrals.

The MC technique is particularly well suited to computing integrals with dimensions greater than ten. Initially, simulations were carried out in the canonical ensemble (keeping N, V and T constant), before extending the technique to other statistical ensembles. In Chapter II, we generate a random sequence of accessible states (Markov chain) in spin models and use simulation methods to explore the configuration space of the system. We sample the regions where the Boltzmann factor is favoured. Consequently, the MC method is generally only useful for the calculation of static properties, since only the configurationally part of the phase space is explored and time is not an explicit variable. Dynamic properties are inaccessible and must be obtained by some other technique.

The Metropolis algorithm is defined by the following states:

- Choose an initial configuration and calculate the initial energy.
- Choose a spin at random
- Attempt to move by reversing this spin.
- We calculate the energy difference ΔE of spin interaction between the new configuration with a flipped spin and the starting configuration.
- If $\Delta E \leq 0$, i.e. the spin reversal decreases the energy, the new configuration is accepted.
- If $\Delta E > 0$: A random number Z is drawn at random according to a uniform distribution.
- If $\boldsymbol{Z} < (-\Delta \boldsymbol{E}/\boldsymbol{kBT})$, we accept the configuration with spin returned as the new configuration. Otherwise it is rejected and the configuration in the next step is identical to the previous configuration.
- The following quantities are calculated: magnetisation per spin, susceptibility per spin, Binder cumulative coefficient, etc.
- We repeat step (2) until convergence.

2.3.2.2. Transfer Matrix Finite-size-scaling m

1. Introduction

Finite-size-scaling (TMFSS) methods and the transfer matrix formalism are an important tool in statistical physics. Historically, they are the ones that made it possible to solve the Ising model in one and two dimensions [71]. They are the basis of exact methods and applications of integrable systems and statistical physics [72]. It is on them that the equivalence between problems of statistical physics and quantum problems is also based. Finally, they allow precise numerical studies [73].

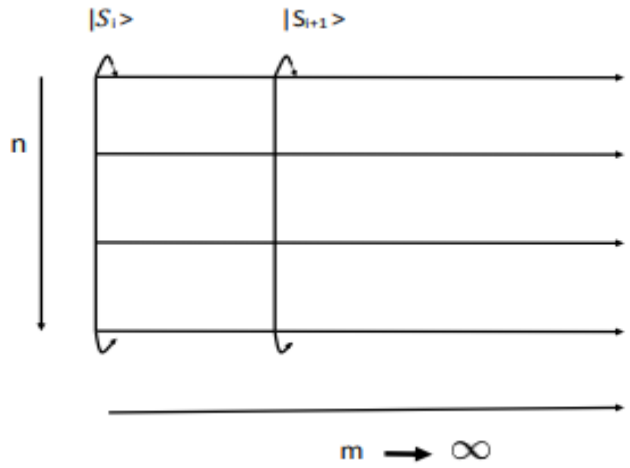

Figure 2.4 ruban de longueur m et de largeur n contenant N spins.

a. Formalism

In the context of a ribbon with a finite width of n and overall length of m, which contains N spins and is subject to periodic edge conditions in the n direction, the transfer matrix T serves as an operator in a vector space. This vector space has a dimension of α_n (where α represents the number of spin states), and is created by the physical configuration of a single layer, represented by the |S> notation.

The given transfer matrix is represented as:

$$T(S_i, S_{i+1}) = \langle S_i|T|S_{i+1}\rangle = e^{-\beta H_i(S_i,S_{i+1})} \tag{2.34}$$

Where $|S_i>$ denotes an Ising spin configuration of the i^{th} layer. The partition function is given by:

$$Z_{n,m} = \sum_{S_i=-1}^{1} \dots \sum_{S_n=-1}^{1} T(S_1, S_2)T(S_2, S_3) \dots T(S_n, S_1) \tag{2.35}$$

By summing over the spins S_2, $S_3 \dots S_n$ we get:

$$Z_{n,m}^{K} = \sum_{S_i=-1}^{1} (T^N)_{S_i,S_i} = trace(T^N) \tag{2.36}$$

Let $\lambda_1 > \lambda_2 > ..... > \lambda_\alpha$ N be the eigenvalues of T, therefore:

$$Z_{n,m}(K) = \sum_{S=1}^{\alpha^N} \left(\lambda_S^{(n)}\right) \approx \left(\lambda_1^{(n)}\right) \quad for\ m \gg 1 \tag{2.37}$$

If $f_n(k)$ is the free energy per spin of an infinite ribbon ($m \to \infty$) and of width n, then :

$$f_n\,(k) = -\lim_{m\to\infty} \frac{1}{nmk} \ln Z_{m,n}(K) = -\frac{1}{nK} \ln \lambda_1^{(n)}\,(k) \tag{2.38}$$

The first two and largest eigenvalues λ_1 and λ_2 of the transfer matrix give the correlation length:

$$[\xi_n(k)]^{-1} = \lim_{m\to\infty} \left[\xi_{n,m}(K)\right]^{-1} = \ln\left[\lambda_1^{(n)}(K)/\lambda_2^{(n)}(K)\right] \tag{2.39}$$

It can be seen that as the size of the ribbon and the spin state vary, the size of the transfer matrix also increases. This makes the elements of the transfer matrix difficult to store, leading to problems with diagonalizing the matrix. For this, the block diagonalization method is used.

b. Block diagonalization

Transformations such as translations and reflections enable physical systems to have a transfer matrix that can be simplified. When it comes to the Ising model, reflecting the system (where $S_i = -S_i$) reduces the matrix from 2^N to 2^{N-1}, but this method does not allow for significant reductions when N becomes large. On the other hand, translations do allow for such reductions.

Suppose that U is a unitary operator that corresponds to the given transformations and it interacts with the same space by commutating with it. The matrix T can be segmented into blocks, each of which corresponds to a distinct eigenvalue of U. As the amount of states is limited, U represents a cyclical transformation of a period L, designated U_L.

The set |I>serves as the foundation for invariants that fall under U_L, and can be attributed to the configurations |S>the I th set of invariants consists of configurations that number N_I, which is always less than or equal to L. As a result, we can express this relationship as follows:

$$|I, j\rangle = U_I^{j-1}|I, 1\rangle \qquad j = 1, \dots, N_I \tag{2.40}$$

Where |I, 1> is chosen to represent an arbitrary element of the I^{th} set, and the other elements are generated by applying the UL transformation. From the members of theI^{TH}set, we construct the U_L Eigen states, defined as follows:

$$U_L\left|I^{(n)}\right\rangle = e^{i(2\pi,L)n}\left|I^{(n)}\right\rangle \tag{2.41}$$

Or

$$n = \begin{cases} -\frac{1}{2}L + 1, \dots, 0, \dots \frac{1}{2}L & For\ L\ is\ pair \\ -\frac{1}{2}L + \frac{1}{2}, \dots, 0; \dots \frac{1}{2}L - \frac{1}{2} & ForL\ is\ impair \end{cases} \quad (2.42)$$

The eigenvectors $|I^{(n)}>$ are given by:

$$\left| I^{(n)} \right\rangle = \frac{\delta(nN_1/L, int)}{N_1^{1/2}} \times \sum_{j=1}^{N_1} e^{-i(2\pi n/L)(j=1)}\, U_L^{j=1} |I; 1\rangle \quad (2.43)$$

Starring:

$$\delta(nN_1/L, int) = \begin{cases} 1 & S_i\ \ nN_1/L\ is\ an\ integer \\ 0 & otherwise \end{cases} \quad (2.44)$$

Now consider an operator $A^{(S)}$, which has well-defined symmetry under the U_L transformation:

$$U_L^+ A^{(S)} U_L = e^{i(2\pi/L)S} A^{(S)} \quad (2.45)$$

Where: $U_L^+ = U_L^{-1}$ is the hermetic conjugate of U_L. The matrix elements of $A^{(S)}$ between the Eigen states $|I^{(n)}>$ of U_L are:

$$\begin{aligned} \left\langle I^{(n)} \middle| A^{(S)} \middle| K^{(m)} \right\rangle &= e^{-i(2\pi/L)S} \left\langle I^{(n)} \middle| U_L^+ A^{(S)} U_L \middle| K^{(m)} \right\rangle \\ &= e^{i\left(\frac{2\pi}{L}\right)(m-n-s)} \left\langle I^{(n)} \middle| A^{(S)} \middle| K^{(m)} \right\rangle \end{aligned} \quad (2.46)$$

With:

$$\left\langle I^{(n)} \middle| A^{(S)} \middle| K^{(m)} \right\rangle = 0 \quad if(m - n - S)/L\ is\ not\ an\ integer \quad (2.47)$$

The transfer matrix T is a special case of an operator $A^{(0)}$, invariant under U_L, hence:

$$\left\langle I^{(n)} \middle| T \middle| K^{(m)} \right\rangle = \delta_{m,n} \left\langle I^{(n)} \middle| T \middle| K^{(n)} \right\rangle \quad (2.48)$$

This relation shows that T is block diagonalizable in the basis n { |I (n) >}.

The symmetrical and anti-symmetrical blocks given by:

T^S and T^A which are the only two blocks that correspond to ordered phases. The largest first eigenvalues of T^S are $\lambda_1^S, \lambda_2^S and \lambda_3^S$ while for T^A the largest eigenvalue is λ_1^A.

The correlation length and persistence length are given by the following equations:

$$\xi_1^A = (\ln|\lambda_1^A/\lambda_1^S|)^{-1} \tag{2.49}$$

$$\xi_1^S = (\ln|\lambda_1^S/\lambda_2^S|)^{-1} \tag{2.50}$$

Respecting the Nightingale argument [74], the exponent ν is obtained by the equation:

$$\upsilon = \ln\left(\frac{N\partial\xi_N^{-1}(K_c)}{\frac{(N+2)\partial\xi_{N+2}^{-1}(K_c)}{\partial T}}\right)\left(\ln\left(\frac{N}{(N+2)}\right)\right)^{-1} \tag{2.51}$$

c. First-order transition.

Phenomenological renormalization is especially suitable for studying second-order transitions where the correlation length diverges. In contrast, for first-order transitions, the condition ξ>>1 is never met. During this type of transition, the matrix's top three eigenvalues hold significance.

When the transfers are degenerate at the limit (N→∞), they correspond to the coexistence of the paramagnetic phase with two ordered phases (up and down ferromagnetic). The degeneracy of the third eigenvector with the largest values provides another constraint that determines the position of the tricritical point along the critical line. This is defined by [75][76]:

$$\hat{\xi}_N = [\ln(\lambda_1/\lambda_3)]^{-1} \tag{2.52}$$

The second correlation length or persistence length is referred to as ξ_N. In finite systems, this degeneration approaches an asymptote that shows a linear increase with a width of N at the triple critical point T = T_t. On the critical point line, the magnetic susceptibility will remain finite, and when (N →∞), it will approach infinity. Therefore, for T > T_t, must be asymptotically unrelated to N.

$$\hat{\xi}_N = A_t N \quad N \to \infty \tag{2.53}$$

$$\hat{\xi}_N = A_2 \quad N \to \infty \tag{2.54}$$

To obtain the behaviour of this quantity along the line formed by first-order transitions for T < T_t, an intuitive argument given by Privman and Fisher can be used. At the first-order transition, the energy required for the formation of an interface across the band is N_σ, where $k_B T_\sigma(T; H)$ is the surface tension of the interface. Hence, the persistence length is a measure of the surface energy between the coexisting phases. The asymptotic behaviour of ξ_N is given by: ξ

$_N$=$A_1Ne^{N\sigma}$ with N→∞. At the tricritical point, σ is zero, generally, the asymptotic behaviour of ξ_N can be expressed as:

$$\hat{\xi}_N = \xi_N^{(reg)} + \begin{cases} A_1 N e^{N\sigma}(1 + B_1 N^{-C1} + \cdots) & For\ T < T_t \\ A_1 N(1 + B_1 N^{-C1} + \cdots) & For\ T = T_t \\ A_2(1 + B_2 N^{-C2} + \cdots) & For\ T > T_t \end{cases} \quad (2.55)$$

Chapter3

3.1. Introduction

This chapter will be devoted to the study of Askhin-Teller model with all that it represents as physical properties. We are interested to ground state by constructing the phase diagrams which will show new thermally stable phases in different regions. By comparing with results already found for this model in previous works, our study differs in introducing spin-3/2.

3.2. Models with spin-3/2

The study of rare earths [77] and mixtures of ternary fluids [78] led to the introduction of the spin-3/2 model. D_yVO_4 is one of the rare earth compounds whose general formula is RVO_4 with a tetragonal structure under room temperature. It orders anti-ferromagnetically in the basal plane at $T_N = 3$ K. Considerations of group theories have shown that this order is only possible if D_yVO_4 has already undergone a change of symmetry. [79] X-ray analysis and specific heat measurements at low temperature have shown the existence of two second-order transitions [80]. One at 14° K (T_D) where D_yVO_4 undergoes a change in symmetry: from tetragonal symmetry to low symmetry. This crystallographic distortion is called the Jahn-Teller transition. The other transition appears at 3 °K (T_N) from the orthorhombic phase to the anti-ferromagnetic phase. We should note that only the quadruplet S = 3/2 participates in the two transitions: at T_D it is separated into two doubles and at T_N into four singlets.

Spin models have allowed us a better understanding of phase transitions in magnetic systems. First introduced by Ising in 1929 to study magnetic transitions, it was not until 1944 that the exact solution was found for a two-dimensional network.

3.2.1. General information on rare earth

Currently, a group of metals known as rare earth elements has gained increasing attention. While some may recognize them as the uppermost row of elements below the main body of the Periodic Table, others may not have heard of them at all. Despite their relative obscurity to the general public until 2009, these metals boast significant applications. The US Geological Survey has stated that rare earth elements (REE) make up the largest chemically cohesive group on the periodic table, and are integral to hundreds of applications. Despite their relative obscurity, the technological, environmental, and economic importance of REE is widely recognized. In the development of modern information, mobility, and energy technologies, a diverse range of functional materials are needed, with rare earths playing a crucial role in even small quantities. This is because their presence is essential to the functionality of the applications [81].

Rare Earth elements are comprised of the lanthanide family and scandium and yttrium. The lanthanide family includes 15 elements with atomic numbers ranging from 57 to 71, while scandium (atomic number 21) and yttrium (atomic number 39) share similar properties and are included in this group [82]. Their electronic structure is the same for the outer layers, with the only variation being an additional electron in the 4f deep layer as we move from one element to the next.

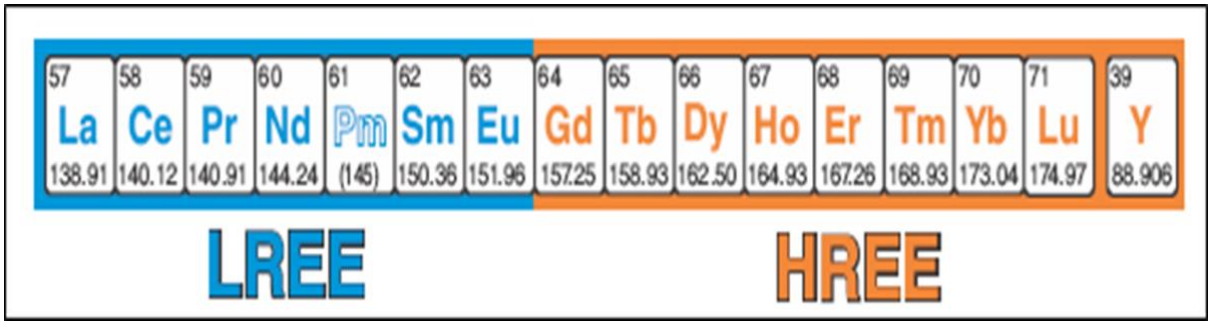

Table 3.1: Periodic table and on black the rare earths

3.2.2. Magnetic characteristics of rare earths

Rare earth elements possess exceptional magnetic properties, with a saturation magnetisation far exceeding that of iron. However, these elements only exhibit magnetic order below room temperature, remaining either paramagnetic or diamagnetic at higher temperatures. To harness the rare earths' magnetic properties, they have been combined with transition metals such as iron, cobalt, or nickel, which possess good magnetic properties and high Curie temperatures (above 400-500C). By doing this, rare earth/transition metal alloys were created, leading to the industrialisation of samarium/cobalt magnets (Tc >700 C). These magnets possess energy density products greater than 0.16 MJ\m^3 for coercive fields of around 800 kA/m, compared to the values of no more than 30 to 50 kJ/m^3 for ferrites or Al-Ni-Co alloys. This breakthrough in miniaturisation has been critical in the development of various devices, such as miniature headphones used with portable music players in the audio-visual sector.

3.3. Study of the (ATM) model

3.3.1. Study of the (ATM) model with spin-1/2

The study of the (ATM) model with spin-1/2 has produced intriguing results. This model has been studied extensively in the field of quantum mechanics as it serves as a simplified representation of a more complex system. The results of the study have shown that the behaviour of the system can be predicted with a remarkable degree of accuracy when using this model. By examining the interactions and movements of condensed matter physics is known to exhibit exotic phases, such as spin liquids and topological states. The use of spin-1/2 particles allows for a more realistic simulation of real-world materials, making the results of this study more pertinent to physical systems. The findings of this model have important implications for the development of new materials with novel properties, such as high-temperature superconductors. The understanding of the complex physics involved in the ATM model with spin-1/2 has shown great potential for advancing not only condensed matter physics but also technology as a whole [83-87].

3.3.2. Study of the (ATM) and spin -1

Using both transfer-matrix Finite-Size-Scaling calculations and Monte Carlo simulations, a comprehensive analysis of the spin-1 Ashkin-Teller model has been conducted. The results of these two numerical methods are qualitatively superior to those that have been obtained through effective Field theory. The phase diagrams in the parameter space (K_4/K_2, D/K_2, T/K_2) show a wide range of phase transitions with surfaces of both first and second-order transitions, which are bounded by lines of tricritical, multicritical, and triple points. Furthermore, for certain values of the four couplings K4/K2 and the anisotropy D/K_2, two partially ordered phases, PO_1 and PO_2, become visible. The spin-1/2 Ashkin-Teller model's PO_1 phase carries over to spin-1 models, while the new PO_2 phase is not present in the usual spin(-1/2) A.T.M.The estimates of the exponent v, calculated through transfer-matrix Finite-Size-Scaling, have revealed a critical line of points belonging to the four-state Potts model for a range of anisotropy values when K_4/K_2 = 1. This is in contrast to only one point of the four-state Potts model in the spin (-1/2)A.T.M. As the model transitions to lower D/K_2, it falls within the Ising tricritical universality class. When the coupling K_4/K_2 strengthens to K4/K2 > 2, calculations of the exponents indicate that the critical lines that separate the F-PO_1 - P and F-PO_2 - P phases fall within the Ising critical and tricritical universality classes. To validate these findings, more accurate estimates of the exponents and a clear definition of the universality of this uncomplicated yet more elaborate model will require the use of more powerful methods such as Monte-Carlo renormalisation and larger sizes [88-91].

3.3.3. Study of the (ATM) model with spin-5/2

A study has been conducted on the ATM (Anisotropic Tensorial Magnetic) model with spin-5/2, and interesting results have been obtained. The ATM model is especially useful in the study of materials with strong magnetic anisotropy, where the magnetic properties depend on the direction of the magnetic field. The examination of the spin-5/2's conduct was the primary focus of this research, which analysed its behaviour under various conditions. Factors like temperature and external magnetic fields were considered in the analysis. The research revealed that the ATM model with spin-5/2 presents unusual magnetic properties due to its high spin value, which creates heterogeneity across time and space scales. The behaviour of the model is heavily influenced by temperature, and a critical temperature was observed to trigger a drastic shift. Furthermore, the study demonstrated that external magnetic field have a considerable impact on the magnetic and thermodynamic properties of the system, giving rise to domains and complex spin configurations. These findings provide valuable insights into the underlying physics of intricate magnetic systems and furnish notable information for practical applications, such as data storage and spintronics [92-97].

3.3.4. Study of the (ATM) model with spin -3\2

3.3.4.1. Model and ground state diagram

The model Hamiltonian is given as follows:

$$H = -K_2 \sum_{\langle ij \rangle} (\sigma_i \sigma_j + S_i S_j) - K_4 \sum_{\langle ij \rangle} (\sigma_i \sigma_j S_i S_j) - D \sum_{\langle i \rangle} (S_i^2 + \sigma_i^2) \qquad (3.1)$$

Where the spins σ_i and S_i are located on sites of a hypercubic lattice and take both the values $\pm$ 3/2 and $\pm$ 1/2. K_2 is the bilinear interaction parameter.K_4 is the four spins interaction parameter. D is the crystal field.

In order to calculate ground state energies, we express the Hamiltonian as a sum of contributions of the nearest-neighbour spins. So the energy per platelet is given as follows:

$$E_P = -K_2(S_a S_b + \sigma_a \sigma_b) - K_4(S_a S_b \times \sigma_a \sigma_b) - D\left(S_i^2 + S_j^2 + \sigma_i^2 + \sigma_j^2\right) \qquad (3.2)$$

- ✓ For small values of K_4/K_2 when $K_4/K_2 < D/K_2$, we have two intervals: If $K_4/K_2 < -0.4$, the spins σ_i are parallel and the spins S_i are antiparallel. Then we have $\langle S \rangle_F = \langle \sigma \rangle_{AF} = \langle \sigma S \rangle_F = 0$ and $\langle S \rangle_{AF} = \langle \sigma \rangle_F = 3/2$. Otherwise, if $K_4/K_2 > -0.4$, the Baxter 3/2 phase is stable because the spins σi and S_i are aligned and equal to 3/2.

- ✓ For intermediate values of K_4/K_2 when $K_4/K_2 > D/K_2$, we have also two regions to consider: If $K_4/K_2 < -4$, the spins σi are parallel and the spins S_i are antiparallel. Then $\langle S \rangle_F = \langle \sigma \rangle_{AF} = \langle \sigma S \rangle_F = 0$ and $\langle S \rangle_{AF} = \langle \sigma \rangle_F = 1/2$ and $\langle \sigma S \rangle_{AF}$, characterize the phase called Baxter - 1/2., otherwise when $K_4/K_2 > -4$, the Baxter 1/2 phase are stable spins σi and S_i are both aligned and equal to 1/2.

- ✓ For large values of K_4/K_2 and except for $K_4/K_2 > D/K_2$, two Baxter mixed phases were found in the range $0 < D/K_2 < -1$, the first when $K_4/K_2 > -0.4$, all spins σ_i and S_i are parallel, and the second when $K_4/K_2 < -0.4$, the spins S_i are parallel while the spins σ_i are misaligned.

The symbols $\langle ... \rangle_F$ and $\langle ... \rangle_{AF}$ denote the thermal average value of the spin variable in the ferromagnetic and antiferromagnetic phases.

3.3.4.2. Results and discussion

Analytically, from equations of the energy per platelet given above, we calculated the different energies of the configurations found by the order of the spin adopted in our work, namely S= 3/2.

From 256 energy equations calculated with different configurations, we have selected those which repeat themselves.. Then we introduced them in a program written in FORTRAN. This code gave us the least energetic and therefore the thermally stable phases. We have grouped the different results and construct a phase diagram of the ground state (T=0).

By comparing the values of the different configurations, we have obtained the following

structure of phase diagram given in figure (3.2) and figure (3.3):

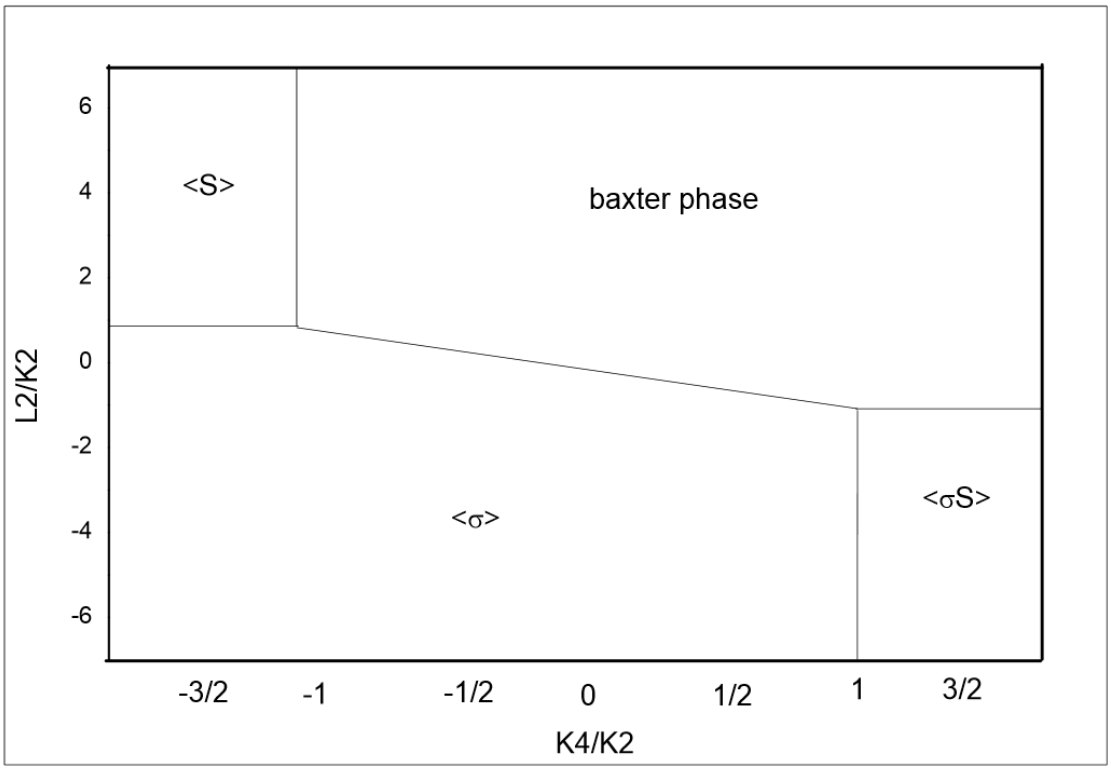

Figure 3.1: Ground state phase diagram for S-1 ATM

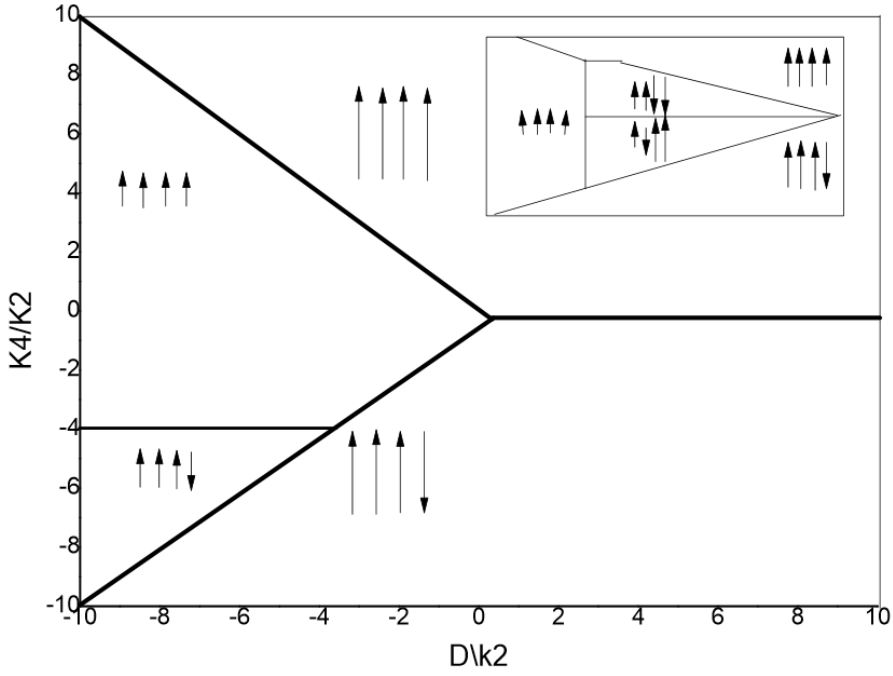

Figure 3.2: Ground state phase diagram for S-3/2 ATM

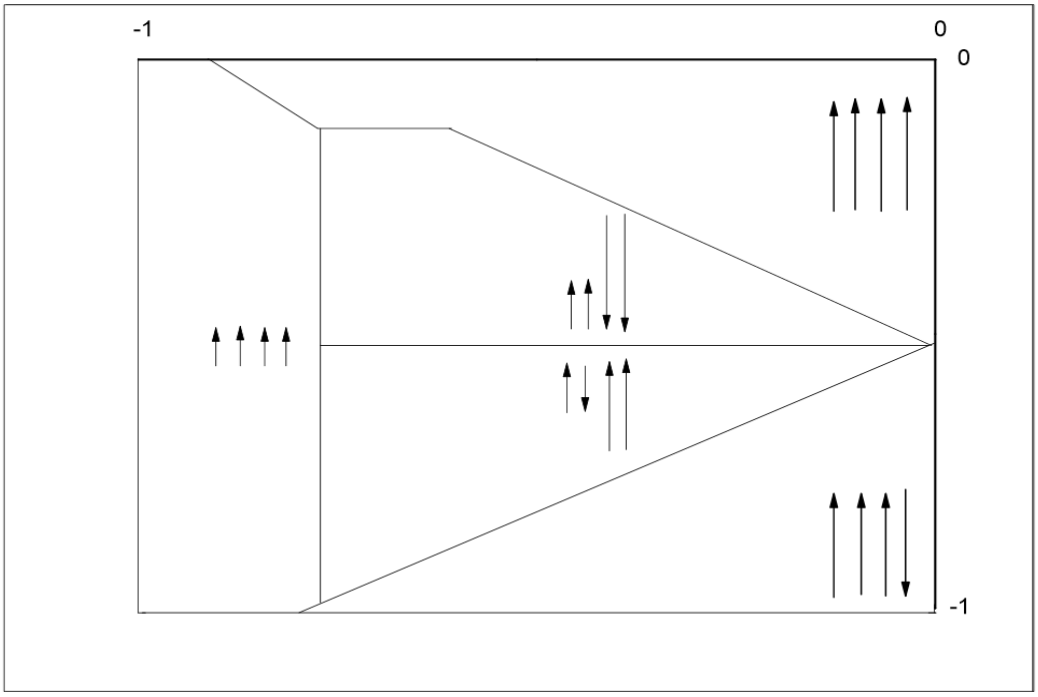

Figure 3.3: Ground state phase diagram for s-3/2 ATM

3.4. Conclusion

After having analytically calculated the different energies of the adopted configurations, the phase diagram of the ground state constructed from the numerical results gave the following results in agreement with the results found by R. Boudefla et al. [98] where we have found a new topology of diagrams formed in comparing them to results of the study of the same models for other different spin values. On another side new thermally stable degenerate phases have appeared in the different regions of this diagram.

General conclusion:

In this modest work, we have studied a lattice spin model of great interest, namely the Askhin-Teller model. Its considers two types of interaction parameters: K_2 for bilinear interactions and K_4 for 4-spin interactions. This model also considers the effect of the crystal field. Specifically we have introduced spin S=3/2 which refers to a very important type of material known as rare earths. After a very long and even sometimes complicated analytical work followed by a carefully done simulation, we had results that we grouped together in a phase diagram designed for the ground state (T=0). We have noticed the appearance of new degenerate phases placed in the different regions of the diagram. In comparison with other previous works, the results also give a new topology of the constructed diagram which provide a database for a probable study of the model at finite temperatures using the different methods of statistical mechanics.

Bibliography references

[1] De Paul D. Beale, Statistical Mechanics, Butterworth-Heinemann, 12 Sept. 1996 - 576 pages.

[2] TOLMAN, Richard Chace. The principles of statistical mechanics. Courier Corporation, 1979.

[3] VAUCLAIR, Sylvie. Eléments de physique statistique. 1993.

[4] YEOMANS, Julia M. Statistical mechanics of phase transitions. Clarendon Press, 1992.

[5] R.K.Pathria,''statistical mechanics'', Second Ed, by Paul D. Beale.

[6] V. R. Ohanyan, L. N. Ananikyan and N. S. Ananikian , Physica A 377 (2007) 501 and references therein.

[7] R. Annequin, J. Boutigny, Electricité 2, 2ime Ed., Eds. Vuilbert, Paris, (1974).

[8] W. E. Hatfield, '' Theory and Applications of Molecular Paramagnetism '', Eds.

E.A. Boudreaux, L. N. Mulay, Wiley New York, (1976) 491

[9] A. Pacault, Rev. Sci., 86, (1948) 38.

[10] P. Pascal, Ann. chim et Phys, (1910) , (1912) , (1913) .

[11] A. Herpin, '' Théorie du magnétisme '', Eds CEA, (1910) 34.

[12] C. Kittel, '' Physique de létat solide '', 7^{ime} Ed., Eds Dunod, Paris, (1998) 379.

[13]Kannan M.Krishnan , "Fundamentals and applications of magnetic materials" ,first edition published in 2016.

[14] DE LACHEISSERIE, Etienne du Tremolet, GIGNOUX, Damien, et SCHLENKER, Michel (ed.). Magnetism. Springer Science & Business Media, 2005.

[15] BLUNDELL, Stephen. Magnetism in condensedmatter. 2003.

[16] PAPON, Pierre, LEBLOND, Jacques, et MEIJER, Paul HE. Physique des Transitions de phases : Concepts et applications. Paris: Dunod, 1999P dunod, paris, france, 1999.

[17] GITTERMAN, Moshe ET HALPERN, Vivian Haim. Phase Transitions: A brief account with modern applications. World Scientific PublishingCompany, 2004.

[18]Robert J.HARDY, CHRISTIEN BINK, thermodynamics and statistical mechanics, 2014 John Wiley & Sons, Ltd.

[19] Gregg laeger, The Ehrenfest classification of phase transitions introduction and evolution, Vol 53. N°1.May1998.P31

[20]ROOS, Yrjo H. ET DRUSCH, Stephan. Phase transitions in foods. Academic Press, 2015.

[21] CHRISTE, Philippe et HENKEL, Malte. Introduction to conformal invariance and its Applications to critical phenomena. Springer Science & Business Media, 2008.

[22]Karson Huang, Introduction to the physics, first published200byTaylor and Francis, 2002.

[23] BARGHATHI, Hatem, HRAHSHEH, Fawaz, HOYOS, José A., et al. Strong-randomness Phenomena in quantum Ashkin–Teller models. Physica Scripta, 2015, vol. 2015, no T165, p. 014040.

[24] MCCOMB, W. David. Study notes for Statistical Physics: A concise, unified overview of the subject-eBooks and textbooks from bookboon. com. 2015.

[25] KUZEMSKY, Alexander Leonidovich. Statistical mechanics and the physics of manyparticle model systems. 2017.

[26] WACHTER, Armin ET HOEBER, Henning. Compendium of theoretical physics. Springer Science & Business Media, 2006.

[27] ZAHIR, H., BAHLAGUI, T., EL KENZ, A., et al. Monte Carlo Study of the Mixed-Spin (1/2, 2) Ferrimagnetic Ising System on a Honeycomb Lattice. Journal of Superconductivity and Novel Magnetism, 2019, vol. 32, no 4, p. 963-970.

[28] AHMED, S. Sidi, BAHMAD, L., BENYOUSSEF, A., et al. mixed spin-1 and spin-1/2 Blume-Emery-Griffiths model on the Bethe lattice: Monte Carlo simulation. Superlattices and Microstructures, 2017, vol. 109, p. 841-851.

[29] MUSSARDO, Giuseppe. Statistical field theory: an introduction to exactly solved models in statistical physics. Oxford University Press, 2010.

[30] Niss, M. History of the Lenz-Ising Model 1920–1950: From Ferromagnetic to Cooperative Phenomena. Arch. Hist. Exact Sci. 59, 267–318 (2005).

[31] BRUSH, Stephen G. History of the Lenz-Ising model. Reviews of modern physics, 1967, vol. 39, no 4, p. 883.

[32] Mattis D.C. (1985) the Ising Model. In: The Theory of Magnetism II. Springer Series

In Solid-State Sciences, vol 55. Springer, Berlin, Heidelberg.

[33] CIPRA, Barry A. An introduction to the Ising model. The American Mathematical Monthly, 1987, vol. 94, no 10, p. 937-959.

[34] NISHIMORI, Hidetoshi ET ORTIZ, Gerardo. Elements of phase transitions and critical Phenomena. OUP Oxford, 2010.

[35] Lars Onsager. Crystal Statistics. I. A Two-Dimensional Model with an Order-Disorder Transition. Phys. Rev., 65 (3):117-149, 1944.

[36] MCCOY, Barry M. et WU, Tai Tsun. The two-dimensional Ising model. Courier Corporation, 2014.

[37] HSU, Elton P. ET VARADHAN, SR Srinivasa (ed.). Probability theory and applications. American Mathematical Soc., 1999.

[38] MARTIN, Paul Purdon. Potts models and related problems in statistical mechanics. World Scientific, 1991.

[39] MUSSARDO, Giuseppe. Statistical field theory: an introduction to exactly solved models in statistical physics. Oxford University Press, 2010.

[40] M.Yezli, Phase transition in the spin-3/2 Blume-Emery-Griffiths model with antiferromagnetic second neighbor interactions, Physica a 448 (2016) 81.

[41] M. Badehdah, S. Bekhechi, A. Benyoussef and M. Touzani, Eur. Phys. J. B 4, (1998) 431.

[42] S. Krinsky and D. Mukamel, Phys. Rev. B 11 (1975) 399. PUG, 1999.

[43] A. Bakchich, S. Bekhechi, A. Benyoussef, Physica A 210 (1994) 415.

[44] S. Bekhechi, A. Benyoussef, Phys. Rev. B 56 (1997) 13954.

[45] YEOMANS, Julia M. Statistical mechanics of phase transitions. Clarendon Press, 1992.

[46] JANSSEN, H. K. From Phase Transitions to Chaos—Topics in Modern Statistical Physics ed G Györgyi et al. 1992.

[47] Ashkin J., Teller E., Phys. Rev., 1943, 64, 178.

[48] Bekhechi S., Benyoussef A., Ettaki B., Loulidi M., Eur. Phys. J. B, 2000, 18, 275–282.

[49] WU, Fa Yueh. Exactly Solved Models: A Journey in Statistical Mechanics-Selected Papers with Commentaries (1963–2008). World Scientific, 2009.

[50] Bezerra C.G., Mariz A.M., de Araujo J.M., da Costa F.A., Physica A, 2001, 292, No. 1 4,429–436.

[51] FRANCISCO, R. M. ET SANTOS, J. P. Magnetic properties of the Ashkin–Teller model on a hexagonal nanotube. Physics Letters A, 2019, vol. 383, no 11, p. 1092-1098.

[52] Kramers H.A., Wannier G.H., Phys. Rev., 1941, 60, No. 3, 252.

[53] Fan C., Phys. Rev. B, 1972, 6, No. 3, 902

[54] Kamieniarz G., Kozłowski P., Dekeyser R., Phys. Rev. E, 1997, 55, No. 3, 3724.

[55] AKINCI, Ümit. Nonequilibrium phase transitions in isotropic Ashkin–Teller model. Physica A: Statistical Mechanics and its Applications, 2017, vol. 469, p. 740-749.

[56] DITZIAN, Ruth V., BANAVAR, Jayanth R., GREST, G. S., et al. Phase diagram for the Ashkin-Teller model in three dimensions. Physical Review B, 1980, vol. 22, no 5, p. 2542.

[57] ARNOLD, Peter ET ZHANG, Yan. Monte Carlo study of very weakly first-order transitions in the three-dimensional Ashkin-Teller model. Nuclear Physics B, 1997, vol. 501, no 3, p. 803-837.

[58] WOJTKOWIAK, Zbigniew ET MUSIAŁ, Grzegorz. Cluster Monte Carlo method for the 3D Ashkin–Teller model. Journal of Magnetism and Magnetic Materials, 2020, vol. 500, p. 166365.

[59] BADEHDAH, M., BEKHECHI, S., BENYOUSSEF, A., et al. Finite-size-scaling study of the anisotropic spin-12 Ashkin–Teller model. Physica B: Condensed Matter, 2000, vol. 291, no 3-4, p. 394-399.

[60] BADEHDAH, M., BEKHECHI, S., BENYOUSSEF, A., et al. Numerical study of the spin-1 Ashkin-Teller model. Physical Review B, 1999, vol. 59, no 9, p. 6250.

[61] BAK, Per, KLEBAN, P., UNERTL, W. N., et al. Phase diagram of selenium adsorbed on the Ni (100) surface: A physical realization of the Ashkin-Teller model. Physical review letters, 1985, vol. 54, no 14, p. 1539.

[62] ZHE, Chang, PING, Wang, ET YING-HONG, Zheng. Ashkin–Teller Formalism for Elastic Response of DNA Molecule to External Force and Torque. Communications in Theoretical Physics, 2008, vol. 49, no 2, p. 525.

[63] GRØNSLETH, M. S., NILSSEN, T. B., DAHL, E. K., et al. Thermodynamic properties near the onset of loop-current order in high-T c superconducting cuprates. Physical Review B, 2009, vol. 79, no 9, p. 094506.

[64] WILLE, L. T. Oxygen ordering and the tetragonalorthorhombic phase transition in YBa2Cu3O7- δ . Phase Transitions: A Multinational Journal, 1990, vol. 22, no 1-4, p. 225 244.

[65] SANTOS, Jander P. et BARRETO, FC Sá. New effective field theory for the Ashkin–Teller model.Physica A: Statistical Mechanics and its Applications, 2015, vol. 421, p. 316 329.

[66] SANTOS, J. P., ROSA, D. S., et BARRETO, FC Sá. New Baxter phase in the Ashkin–Teller model on a cubic lattice. Physics Letters A, 2018, vol. 382, no 5, p. 272-275.

[67] BAHMAD, L., BENYOUSSEF, A., ET EZ-ZAHRAOUY, H. Anisotropic Ashkin-Teller Model in a Transverse Field. physica status solidi (b), 2001, vol. 226, no 2, p. 403-411.

[68] DE OLIVEIRA, Paulo Murilo C. et BARRETO, FC Sá. Renormalization group studies of the Ashkin-Teller model. Journal of Statistical Physics, 1989, vol. 57, no 1-2, p. 53-63.

[69] M.Heritier, Mécanique statistique et transitions de phase, DEA, région parisienne, (1998).

[70] N. Metropolis ET S. Ulam, the monte carlo method, Journal of the American Statistical Association, 44 (1949) 335

[71] Metropolis, N., Rosenbluth, A.W., Rosenbluth, M.N., Teller, A.H., and Teller, E. Equation of State Calculations by Fast Computing Machines, Journal of Chemical Physics, 21(6), 1087-1092 (1953).

[72] BERG, B. A. et SIMULATIONS, Markov Chain Monte Carlo. Their Statistical Analysis with Web-Based FORTRAN Code, Ⅱ. 2004.

[73] HITCHCOCK, David B. A history of the Metropolis–Hastings algorithm. The American Statistician, 2003, vol. 57, no 4, p. 254-257.

[74] HAYOUN, Marc. La méthode de monte carlo metropolis. École « Simulation Numérique en Matière Condensée » (Paris, 29-31 mai 2002), 2002.

[75] A. E. Ferdinand et M. E. Fisher, Phys. rev. 185 (1969) 832

[76] M.P. Nightingale, Physica 83 A, 561(1976); Phys. Lett. 59 A (1977) 486; J. Appl. Phys. 53 (1982) 7927.

[77] C. Domb, Adv. Phys. 9 (1960) 149.

[78] P.A. Rikvold, W. Kinzel, J.D. Gunton et K. Kaski, Phys. Rev. B 28 (1983) 2686

[79] P.D. Beale, Phys. Rev. B 33 (1986) 1717.

[80] A.H. Cooke, D.M. Martin and M.R. Wells, J. Phys.(Paris) C1 (1971) 488.

[81] S. Krinsky and D. Mukamel, Phys. Rev. B 11 (1975) 399.

[82] A.H. Cooke, D.M. Martin and M.R. Wells, Solid State Communications, Vol. 09 (1971) 519.

[83] A.H. Cooke, D.M. Martin and M.R. Wells, Solid State Communications, Vol. 08 (1970) 689

[84]S.Yen. China and Geopolitics of rare earth. Springer. (2019)

[85]J.Smith.Rare Earth Elements: Properties, Applications and Future prospects. Springer, 2018.

[86] National Institute of Health. (2020). PubMed Central. Retrieved from https://www.ncbi.nlm.nih.gov/pmc/.

[87] American Medical Association. (2020). AMA Manual of Style. Retrieved from https://www.amamanualofstyle.com/

[88] Harvard Library. (2020). Harvard Referencing. Retrieved from https://guides.library.harvard.edu/referencing

[89] Oxford University Press. (2020). Oxford Referencing. Retrieved from https://www.ox.ac.uk/students/academic/guidance/skills/plagiarism?wssl=1

[90] M. P. M. denNijs, J. Phys. A 12, 1857 (1979)

[91] B. Nienhuis, E. K. Riedel and M. Schick, J. Phys. A 13, L 189 (1980).

[92] H. E. Stanley, Introduction to Phase Transitions and Critical Phenomena. (Oxford University Press, Oxford 1971).

[93] B. M. McCoy and T. T. Wu, The Two dimensional Ising Model. (Harvard University Press, Cambridge, MA, 1973).

[94]Alexandre Zagoskin "The Kondo-Anderson model: Physics at the nanoscale". (2006).

[95] Harold U. Baranger and William B. "Electronic transport through single molecules" Thormann (2001).

[96] M. V. Gurudev Dutt et al. "Decoupling of electronic and nuclear spin qubits by coherent dynamical manipulation of quadrupolar nuclei". (2007).

[97] J. Martinek et al ."Kondo effect and spin-dependent tunneling in magnetic nanostructures".(2003).

[98] R. Boudefla et al., Cond. Mat. Phys. Vol. 18 N0 3 (2015).